ABSTRACT

Title of Thesis:	IDENTIFICATION OF HUMAN WALKING PATTERNS USING 3D-DYNAMIC MODELING
	Kaustav Nandy, Master of Science, 2006
Thesis Directed By:	Professor. Rama Chellappa Department of Electrical And Computer Engineering

One of the most common activities of our day to day life is walking. However simulating a human walking motion is one of the most difficult tasks to accomplish. Inherently it is an inverted pendulum like system and involves a large number of degrees of freedom. In this thesis we have modeled the human walking motion. The system is designed using a human body model in the form of a kinematic chain consisting of rigid links and revolute joints. Human walking patterns contain information like identity, presence of physical disability and loading conditions of a person like carrying a backpack. We have extracted some of these information and have used our model to discriminate various walking motions. The information that we have used are joint torque and angle sequences modeled using ARMA modeling and Dynamic Time Warping. Our human walking model is validated by comparing it with Stanford marker data.

IDENTIFICATION OF HUMAN WALKING PATTERNS USING 3-D DYNAMIC MODELING

by

Kaustav Nandy

Thesis submitted to the Faculty of the Graduate School of the
University of Maryland, College Park, in partial fulfillment
of the requirements for the degree of
Master of Science
2006

Thesis Advisory Committee:

Professor. Rama Chellappa, Chairman/Advisor
Professor. Carol Y. Espy-Wilson
Dr. Qinfen Zheng

Dedicated To

My Parents . . .

ACKOWLEDGEMENTS

I am extremely grateful to my advisor, Dr. Rama Chellappa for his constant support and encouragement. He has always been a constant source of inspiration for me throughout this work. I would also like to thank Dr. Carol Y. Espy-Wilson and Dr. Qinfen Zheng for being on my thesis defense committee. I am thankful to Mr. Aravind Sundaresan and Mr. Ashok N. Veeraraghavan for discussing with me various issues about my work and also providing with some of their suggestions. I would like to take this opportunity to thank my roommates and friends who made my stay at Maryland very enjoyable.

Contents

List of Figures **vi**

List of Tables **xi**

1 Introduction **1**
1.1 Motivation 1
1.2 Previous Work 4
1.3 Contribution 5
1.4 Organization Of The Thesis 6

2 Human Body Model and the Motion Model **7**
2.1 Human Body Characteristics 7
2.2 Articulated Human body model 9
2.3 General Human Motion Model 13

3 The Inverse and Forward Dynamics Modeling **15**
3.1 System Overview 15
3.2 Inverse Dynamics 17
3.2.1 Outward Loop 18
3.2.2 Inward Loop 19
3.2.3 Simulation of the Inverse Dynamics System 20
3.3 Forward Dynamics 20
3.3.1 Simulation and Visualization of the Forward Dynamics System 22
3.3.2 Controller for Forward simulation 23
3.4 Modeling of Angle and Torque vectors 23
3.4.1 ARMA Modeling 23
3.4.2 Dynamic time warping 25

4 Data, Experiments and Results **26**
4.1 The Stanford Marker Data 27

4.2 Discrimination of Walking Patterns 28
4.2.1 Results 30
4.2.2 Discussion 39
4.3 Simulation of Walking Patterns 39
4.3.1 Results 41
4.3.2 Discussion 48
4.4 Validation of the Model with the marker data 48
4.4.1 Results 49
4.4.2 Discussion 52

5 Conclusion and Future Work **53**

Bibliography **55**

List of Figures

2.1 Average human body dimensions of an U.S. male. The dimensions are shown in inches. 8
2.2 Kinematic linked structure used to model the human body. The individual links are connected by revolute joints of one degree of freedom. . . 9
2.3 Figure shows the sagittal plane(green) of the human body 10
2.4 Figure shows a revolute joint 11
2.5 The complete human model along with ground connection 12
2.6 Figure shows the different states of human walking 13

3.1 Block diagram of the human motion generation system 16
3.2 Complete human model developed using the SimMechanics toolbox (a) Convex Hull visualization (b) Equivalent ellipsoid visualization 22

4.1 Few screenshots of the Stanford Marker Data 27
4.2 The plots of angle data input to the inverse dynamics system block for a single gait cycle. Angle between (a) Ground and the shin of the support leg (b) Right shin and right thigh (c) Right thigh and torso (d) Left thigh and torso (e) Left thigh and shin (f) Torso and left upper arm (g) Left upper arm and lower arm (h) Torso and right upper arm (i) Right upper arm and lower arm 30
4.3 The plots of torque data which is the output of the inverse dynamics system block for a single gait cycle. Torque of joint between (a) Ground and the shin of the support leg (b) Right shin and right thigh (c) Right thigh and torso (d) Left thigh and torso (e) Left thigh and shin (f) Torso and left upper arm (g) Left upper arm and lower arm (h) Torso and right upper arm (i) Right upper arm and lower arm (j) Torso and neck (k) Neck and head 31

4.4 The plots of angle data for a normal human, human with a backpack and a limping human, input to the inverse dynamics system block for a single gait cycle. Angle between (a) Ground and the shin of the support leg (b) Right shin and right thigh (c) Right thigh and torso (d) Left thigh and torso (e) Left thigh and shin (f) Torso and left upper arm (g) Left upper arm and lower arm (h) Torso and right upper arm (i) Right upper arm and lower arm 32
4.5 The plots of torque data of a normal human, human with backpack and a limping human, which is the output of the inverse dynamics system block for a single gait cycle. Torque of joint between (a) Ground and the shin of the support leg (b) Right shin and right thigh (c) Right thigh and torso (d) Left thigh and torso (e) Left thigh and shin (f) Torso and left upper arm (g) Left upper arm and lower arm (h) Torso and right upper arm (i) Right upper arm and lower arm (j) Torso and neck (k) Neck and head 33
4.6 The plots of angle data for a normal human, human with a backpack and a limping human, input to the inverse dynamics system block for a single gait cycle and 5 different individuals. Angle between (a) Ground and the shin of the support leg (b) Right shin and right thigh (c) Right thigh and torso (d) Left thigh and torso (e) Left thigh and shin (f) Torso and left upper arm (g) Left upper arm and lower arm (h) Torso and right upper arm (i) Right upper arm and lower arm 34
4.7 The plots of torque data of a normal human, human with a backpack and a limping human, which is the output of the inverse dynamics system block for a single gait cycle and 5 different individuals. Torque of joint between (a) Ground and the shin of the support leg (b) Right shin and right thigh (c) Right thigh and torso (d) Left thigh and torso (e) Left thigh and shin (f) Torso and left upper arm (g) Left upper arm and lower arm (h) Torso and right upper arm (i) Right upper arm and lower arm (j) Torso and neck (k) Neck and head 35
4.8 The similarity matrix of the angle data using ARMA modeling and gap distance. First 20 are normal, next 20 are with backpack and the last 20 correspond to limping sequences 36
4.9 The similarity matrix of the torque data using ARMA modeling and gap distance. First 20 are normal, next 20 are with backpack and the last 20 correspond to limping sequences 36
4.10 The similarity matrix of the angle data using ARMA modeling and Frobenius distance. First 20 are normal, next 20 are with backpack and the last 20 correspond to limping sequences 37

4.11 The similarity matrix of the torque data using ARMA modeling and Frobenius distance. First 20 are normal, next 20 are with backpack and the last 20 correspond to limping sequences 37
4.12 The similarity matrix of the angle data using dynamic time warping. First 20 are normal, next 20 are with backpack and the last 20 correspond to limping sequences 38
4.13 The similarity matrix of the torque data using dynamic time warping. First 20 are normal, next 20 are with backpack and the last 20 correspond to limping sequences 38
4.14 Plots of angle data output of the forward dynamics system block for a single gait cycle. Angle between (a) Ground and the shin of the support leg (b) Right shin and right thigh (c) Right thigh and torso (d) Left thigh and torso (e) Left thigh and shin (f) Torso and left upper arm (g) Left upper arm and lower arm (h) Torso and right upper arm (i) Right upper arm and lower arm 41
4.15 Plots of torque data which are input to the forward dynamics system block for a single gait cycle using the controller. Torque of joint between (a) Ground and the shin of the support leg (b) Right shin and right thigh (c) Right thigh and torso (d) Left thigh and torso (e) Left thigh and shin (f) Torso and left upper arm (g) Left upper arm and lower arm (h) Torso and right upper arm (i) Right upper arm and lower arm (j) Torso and neck (k) Neck and head 42
4.16 Plots of angle data for a normal human, human with a backpack and a limping human, output of the forward dynamics system block for a single gait cycle. Angle between (a) Ground and the shin of the support leg (b) Right shin and right thigh (c) Right thigh and torso (d) Left thigh and torso (e) Left thigh and shin (f) Torso and left upper arm (g) Left upper arm and lower arm (h) Torso and right upper arm (i) Right upper arm and lower arm 43
4.17 Plots of torque data of a normal human, human with backpack and a limping human, which are output to the inverse dynamics system block for a single gait cycle using the controller. Torque of joint between (a) Ground and the shin of the support leg (b) Right shin and right thigh (c) Right thigh and torso (d) Left thigh and torso (e) Left thigh and shin (f) Torso and left upper arm (g) Left upper arm and lower arm (h) Torso and right upper arm (i) Right upper arm and lower arm (j) Torso and neck (k) Neck and head 44

4.18 The similarity matrix of the angle data using ARMA modeling and Frobenius distance. The first column corresponds to normal walking simulation, the second and the third correspond to walking with a backpack and the last two correspond to limping. 45
4.19 The similarity matrix of the torque data using ARMA modeling and Frobenius distance. The first column corresponds to normal walking simulation, the second and the third correspond to walking with a backpack and the last two correspond to limping. 45
4.20 The similarity matrix of the angle data using ARMA modeling and Gap distance. The first column corresponds to normal walking simulation, the second and the third correspond to walking with a backpack and the last two correspond to limping. 46
4.21 The similarity matrix of the torque data using ARMA modeling and Gap distance. The first column corresponds to normal walking simulation, the second and the third correspond to walking with a backpack and the last two correspond to limping. 46
4.22 The similarity matrix of the angle data using Dynamic time warping. The first column corresponds to normal walking simulation, the second and the third correspond to walking with a backpack and the last two correspond to limping. 47
4.23 The similarity matrix of the torque data using Dynamic time warping. The first column corresponds to normal walking simulation, the second and the third correspond to walking with a backpack and the last two correspond to limping. 47
4.24 The similarity matrix of the angle data of the forward dynamics simulation and the actual marker data using ARMA modeling and Frobenius distance. The first column corresponds to normal walking simulation, the second and the third correspond to walking with a backpack and the last two correspond to limping. The rows correspond to the sixty data sequences. First 20 are normal, next 20 are with backpack and the last 20 are limping sequences. 49
4.25 The similarity matrix of the torque data of the forward dynamics simulation and output of the Inverse dynamics simulation using ARMA modeling and Frobenius distance. The first column corresponds to normal walking simulation, the second and the third correspond to walking with a backpack and the last two correspond to limping. The rows correspond to the sixty data sequences. First 20 are normal, next 20 are with backpack and the last 20 are limping sequences. 50

4.26 The similarity matrix of the angle data of the forward dynamics simulation and the actual marker data using ARMA modeling and Gap distance. The first column corresponds to normal walking simulation, the second and the third correspond to walking with a backpack and the last two correspond to limping. The rows correspond to the sixty data sequences. First 20 are normal, next 20 are with backpack and the last 20 are limping sequences. 50
4.27 The similarity matrix of the torque data of the forward dynamics simulation and output of the inverse dynamics simulation using ARMA modeling and Gap distance. The first column corresponds to normal walking simulation, the second and the third correspond to walking with a backpack and the last two correspond to limping. The rows correspond to the sixty data sequences. First 20 are normal, next 20 are with backpack and the last 20 are limping sequences. 51
4.28 The similarity matrix of the angle data of the forward dynamics simulation and the actual marker data using DTW. The first column corresponds to normal walking simulation, the second and the third correspond to walking with a backpack and the last two correspond to limping. The rows correspond to the sixty data sequences. First 20 are normal, next 20 are with backpack and the last 20 are limping sequences. . 51
4.29 The similarity matrix of the torque data of the Forward dynamics simulation and output of the Inverse dynamics simulation using Dynamic time warping. The first column corresponds to Normal walking simulation, the second and the third correspond to walking with a backpack and the last two correspond to limping. The rows correspond to the sixty data sequences. First 20 are normal, next 20 are with backpack and the last 20 are limping sequences. 52

List of Tables

2.1 Human body weight distribution 8
2.2 Different model joints. All joint axes are orthogonal to the sagittal plane. 11
2.3 Model body weight and length distributions. 12

4.1 Data used in our experiments 28

Chapter 1

Introduction

1.1 Motivation

Walking is one of the most common activities performed by humans. But the process of analyzing and simulating human gait is one of the most difficult problems to handle. Inherently it is an inverted pendulum like system and also involves a large number of degrees of freedom. Various methods have been employed for the purpose of human motion analysis for human recognition, abnormality detection and also medical purposes like monitoring knee recovery after surgery. Human locomotion simulation is largely studied in the fields of computer animation, biomechanics, robotics and also computer vision.

Human walking patterns can provide very rich and detailed information. Just by looking at the walking motion of a person we can detect whether he or she is happy, has some physical disability or even tired. In most of the cases we can also predict gender of a person. If the person is someone we know we can also recognize him or

her by observing the way he or she walks. Certainly all of these pieces of information are encoded in the walking patterns of all humans. However we can also say that they are not included in a specific frame, but we have to look at the dynamics of the walking process. We might not be able to say that a person is hurt or not from a single image, but if we are presented with a video sequence of a walking person, we can very easily infer about the pieces of information mentioned above.

In this work we are attempting to capture the variations in human walking due to different loadings of the human body. By looking at a walking person we can usually infer whether he or she is carrying a backpack or not. The loading conditions can be carrying a heavy backpack or having something strapped to the chest or leg. We want to analyze the effect of these loadings on human walking through the use of a dynamic model for human locomotion.

The use of a dynamical model has been motivated by the idea that the information that we are looking for is largely encoded in the dynamics of human motion. We can capture human gait variations and discriminating features in the joint angle and joint torque variations with time. Hence we largely concentrate at the time variations and evolutions of joint angles and torques of a person and try to predict whether he or she has some abnormality in his or her gait pattern.

The problem has been divided into two subproblems, namely

1. ***Inverse Dynamics to get the joint torques***: The inverse dynamics problem [27] [28] [29] is of solving the joint torques from the joint angles along with their first and second order derivatives. This problem can be solved in several ways. In this

work we have used the Newton-Euler recursive algorithm [27].

2. ***Forward Dynamics***: This problem estimates the joint angles from joint torques. This is done by representing the human body motion in the form of a differential equation and then numerically integrating the equation. The general differential equation of motion that arises in this problem is shown below.

$$\tau = M(\Theta)\ddot{\Theta} + V(\Theta, \dot{\Theta}) + G(\Theta) \tag{1.1}$$

This equation represents [27] the general case of a dynamic model that includes the model we have used.

The main applications of the systems can also be divided into two categories.

- Using the inverse dynamics algorithm we can find the joint torques of a human from the joint angles. Then we can use these joint torque values to identify whether a person is walking normally or abnormally. Also we can detect whether a person is carrying some load on his body or not.

- Using the forward dynamics algorithm we can generate different types of gait patterns. This validates the correctness of the model. It also helps us to generate gait patterns when a person is carrying something on this back or strapped to his chest or leg.

1.2 Previous Work

Human gait has been a subject of interest in many fields like computer animation, biomechanics, robotics and computer vision.

Specially in computer animation, human motion generation is an area where a lot of work has been done [1]. [2] [3] [4] [5] [6] have developed models which are physically realistic. These models takes into account all the different physical constraints like gravity, surrounding environmental forces and also body muscle torques. In general, the problem with these methods is that even if all the physical forces have been taken into account, synthesized movement is not realistic. In this context we must mention [30], which contains algorithms to simulate, analyze and generate human motion. The alternative to this is the use of kinematic methods [7] [8]. In this method the kinematics data is captured and used for generating the animation. But the problem with kinematic method of human motion generation is generalization for different types of situations. In this context we must mention the method used by Ko and Badler [9] [10] [11] for generalizing gait data. In their method there is a post processing step that checks the feasibility of the pattern generated. Their generalization was across stride length and also curved path locomotion. They have also showed that their model can be used to generate gait patterns under different loading conditions. All these methods use some biomechanical knowledge and some previously collected gait data for the generalization purpose. Sun and Metaxas have combined these methods in [12].

In the robotics community bipedal locomotion is a very popular topic and we can find several works on the same. In general a biped can be represented as an inverted

pendulum system. This system under goes a constrained motion due to the impact of the swing leg and the ground [13] [14]. In this context [13] provides a survey of modeling and control of bipedal locomotion systems. [15] presents a motion control framework that uses virtual components and robot control is achieved via the forces of interaction between these virtual components and the robot. They have applied the algorithm for the control of a planar bipedal robot. In [16] Chew and Pratt have explored the performance of the algorithms under different load variations and have proposed a robust adaptive controller to be used along with the "Turkey Walking" algorithm. Parseghian [17] presents a physically-based control method for a three-dimensional bipedal robot which can leans sideways, pickup its foot and start walking. [18] presents an approach for deriving control system models for different phases of the walking cycle, both single support and double support phase. They deal with the holonomic constraints and the ground reaction forces involved with the process of human walking.

Computer vision mainly uses human gait for recognition of humans. There are two types of methods, appearance based and model based. Appearance based models can be deterministic [19] [20] or stochastic using a hidden Markov Model (HMM) [21] [22].

1.3 Contribution

In this work we have captured the variations of human motion using a 3-D dynamic model. We have tried to discriminate human walking patterns under different loading conditions of the human body, like carrying a backpack or having something strapped to the chest or leg, using the angle and torque vector sequences. We have also simulated different gait patterns under loading conditions using our model. To the best of our

knowledge discriminating human gait patterns using the angle and torque is a new work and has not been reported before. Also we have validated the model by showing that the output of the model in the forward dynamics simulation closely matches the real human motion data.

1.4 Organization Of The Thesis

The organization of this thesis is as follows. In this chapter we have provided an introduction to the problem along with the previous work done in this area. Chapter 2 presents a detailed description of the human body model and the motion model that we have used in our work. The inverse and forward dynamics algorithms used have been described in chapter 3. The results of the inverse and forward dynamics experiments are summarized in chapter 4. Finally chapter 5 contains the conclusions and future work.

Chapter 2

Human Body Model and the Motion Model

The human body model used in this work is a kinematic chain of rigid links. A detailed description of the model is provided in this section.

2.1 Human Body Characteristics

In order to simulate or analyze human motion using a dynamic model we need to take a look at the general human body characteristics [23] [24]. These body characteristics when incorporated into the model makes it more authentic and realistic. Since we are aiming at discriminating human motion using our model, it is essential that we capture the details of the human body characteristics.

Among the body characteristics the ones that are most important to us are the weight distribution and the average dimensions of a human body. The following table shows

the weight distribution of an average human body [25]. It can be noticed that most of the body mass is above the waist height.

Body Parts	Mass Percentage per parts	Number of Parts	Total mass percentage
Head, Neck, Torso	31%	1	31%
Hands	5%	2	10%
Pelvis, Abdomen	27%	1	27%
Thigh	10%	2	20%
Shin, Foot	6%	2	12%

Table 2.1: Human body weight distribution

The following figure shows the average human body dimensions. The center of gravity of the structure is at an height of about $38''$, which is just above the hip [23].

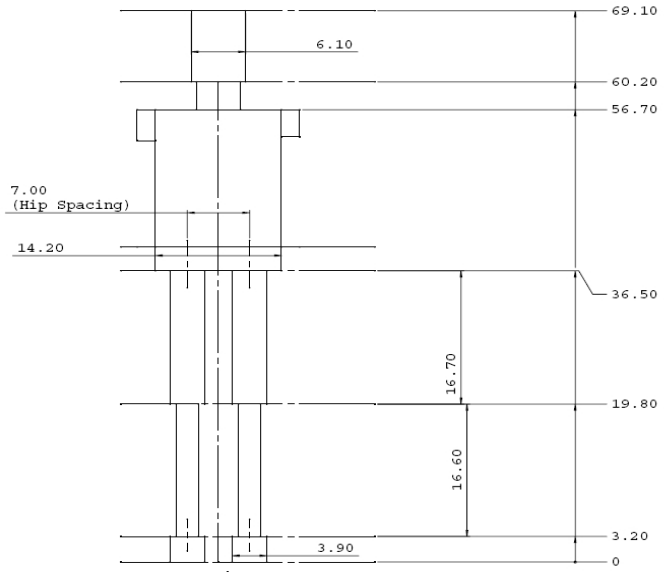

Figure 2.1: Average human body dimensions of an U.S. male. The dimensions are shown in inches.

We have incorporated information on human body dimensions to make our analysis more thorough and realistic. The next section provides a detailed description of the

model that we use.

2.2 Articulated Human body model

We have modeled the human body as a kinematic chain of rigid links. This type of a model has been used earlier in [26], but with a different purpose. There are in all 11 links. The links are left lower leg, left upper leg, right lower leg, right upper leg, torso, left upper arm, left lower arm, right upper arm, right lower arm, neck and head. The stick figure is shown below in figure 2.2. All the links are assumed to be perfectly rigid with zero diameter. The center of mass of the links are at the center of length.

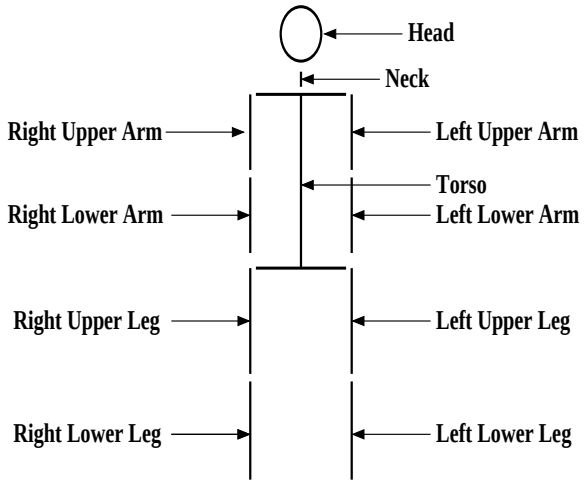

Figure 2.2: Kinematic linked structure used to model the human body. The individual links are connected by revolute joints of one degree of freedom.

The junctions of the links are connected in general by spherical joints which can rotate about all the three axes i.e. have 3 - degrees of freedom. Hence in general the total number of degrees of freedom with 11 joints is 33. In this work we have constrained

the motion of the model in the sagittal plane i.e. the plane passing through the center line of a human body and divides the body symmetrically into two equal halves. Hence the joints are modeled using revolute joints having their axis of rotation in the plane perpendicular to the sagittal plane. The sagittal plane is shown in figure 2.3.

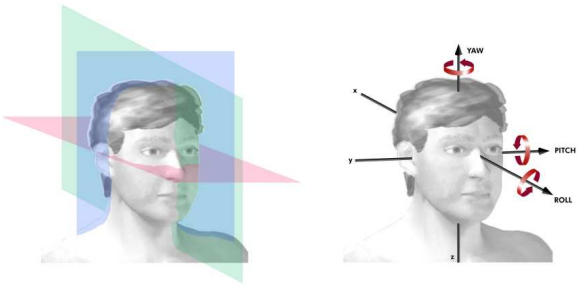

Figure 2.3: Figure shows the sagittal plane(green) of the human body

The total number of degrees of freedom for the body model is then 10, and all the DOF's correspond to a revolute joint. A revolute joint is shown in figure 2.4. We have added another degree of freedom to the stance leg where the leg rests on the ground. We have modeled the body ground joint as a revolute joint and torque is applied to this joint to move the body forward. All the above joints mentioned are actuated joints and appropriate torque is applied to the joints to generate the human motion. Hence the total number of DOF of the model is 11, since their rotation is confined only to the sagittal plane. A posture of the model can now be described using the following angle vector $\Theta \triangleq [\theta_1 \quad \theta_2 \quad \theta_3 \quad \theta_4 \quad \theta_5 \quad \theta_6 \quad \theta_7 \quad \theta_8 \quad \theta_9 \quad \theta_{10} \quad \theta_{11}]^T$. Similarly the torques applied to the 11 joints can be described by $\tau \triangleq [\tau_1 \quad \tau_2 \quad \tau_3 \quad \tau_4 \quad \tau_5 \quad \tau_6 \quad \tau_7 \quad \tau_8 \quad \tau_9 \quad \tau_{10} \quad \tau_{11}]^T$

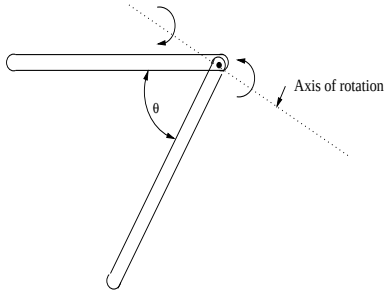

Figure 2.4: Figure shows a revolute joint

These vectors are used in computation of the forward and the inverse dynamics of the model. The angle vectors are the inputs to the inverse dynamics system and the output are the torque vectors. While the forward dynamics system takes the torque vectors as input and produces the angle vectors as the outputs.

The following table shows the different joints in the model along with their symbols and degrees of freedom.

Joint Name	Joint Angle Symbol	Joint Torque Symbol	Joint DOF
Stance Leg and Ground	θ_1	τ_1	1
Stance Leg Knee	θ_2	τ_2	1
Stance Leg Hip	θ_3	τ_3	1
Swing Leg Hip	θ_4	τ_4	1
Swing Leg Knee	θ_5	τ_5	1
Swing Leg side Shoulder	θ_6	τ_6	1
Swing Leg side Elbow	θ_7	τ_7	1
Stance Leg side Shoulder	θ_8	τ_8	1
Stance Leg side Elbow	θ_9	τ_9	1
Neck and Torso	θ_{10}	τ_{10}	1
Neck and Head	θ_{11}	τ_{11}	1

Table 2.2: Different model joints. All joint axes are orthogonal to the sagittal plane.

The next table shows the different parts of the model along with their mass distribution

and length distribution. These values are representative and can be changed very easily accordingly if the situation demands.

Model Parts (Links)	Mass in metric system	Length in metric system
Left and Right shin	5	0.4
Left and Right thigh	10	0.5
Torso	20	vertical: 0.5 Horizontal: 0.3
Left and Right upper arm	3	0.3
Left and Right lower arm	2	0.3
Neck	5	0.1
Head	10	Diameter: 0.2

Table 2.3: Model body weight and length distributions.

Figure 2.5 shows the complete human model that we have used in our work along with the ground connection modeled as a revolute joint

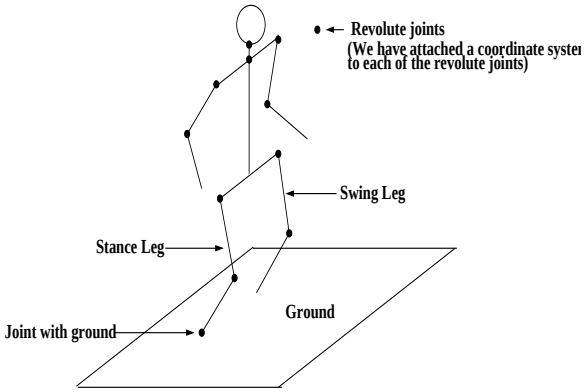

Figure 2.5: The complete human model along with ground connection

The next section provides a description of the motion model used in our work.

2.3 General Human Motion Model

We have adopted the following human motion model which has been used in previous works [26]. In general, human motion can be described by three states and the body goes through all these states periodically. As the states are visited periodically, the human gait is generated. The states are

Double Support In this state the body is supported by both the legs

Right Support In this state the body is supported by the right leg (*support leg*) only and the left leg is the *swing leg*

Left Support In this state the body is supported by the left leg (*support leg*) only and the right leg is the *swing leg*

The following figure shows the three states and the sequence in which the states are visited.

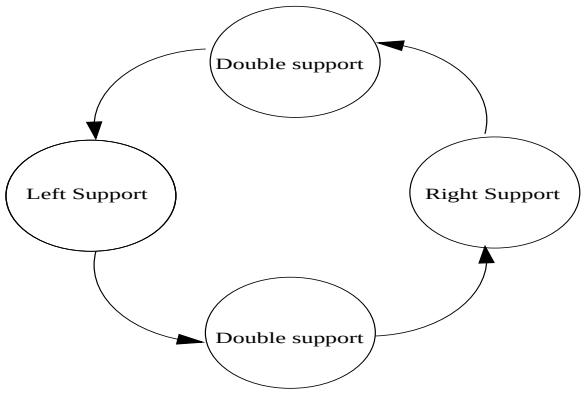

Figure 2.6: Figure shows the different states of human walking

In this work we have assumed that the time duration of the double support phase is very small and the transition from the left support to the right support or from the

right support to the left support is instantaneous. In fact the simulation of this system alternates between the two phases.

Chapter 3

The Inverse and Forward Dynamics Modeling

This chapter provides a description of the entire system that we have developed along with the algorithms used.

3.1 System Overview

In figure 3.1 the entire system is described. Initially, the joint angle data is manually extracted from a video sequence by hand marking the points of interest in the video frames or as in our case, marker data collected in Stanford Biomotion Lab is used to locate the joint positions of a human body. The points of interest for our case are the body joints like the ankle, knee, hip, shoulder, elbow etc, so that we can compute the angles made by the links connected to the joint. The extraction of the joint angles is done by the application concepts of 3-D geometry. Since the motion of the model joints has been confined to one dimension only, the angles that are calculated

are on the sagittal plane. As a result of this calculation for each frame we capture the posture of the human model or the data in terms of the 11-dimensional angle vector $\Theta \triangleq [\theta_1 \quad \theta_2 \quad \theta_3 \quad \theta_4 \quad \theta_5 \quad \theta_6 \quad \theta_7 \quad \theta_8 \quad \theta_9 \quad \theta_{10} \quad \theta_{11}]^T$ as we have already mentioned.

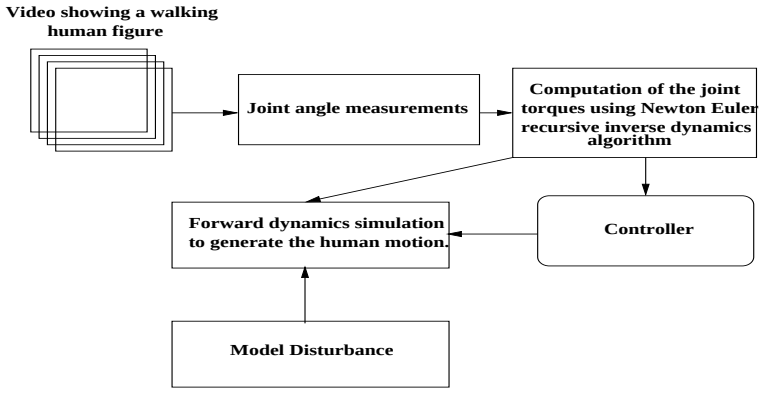

Figure 3.1: Block diagram of the human motion generation system

The process of calculating the joint angles is represented by the block shown as "Joint Angle Measurement". These joint angle measurements are then fed to the inverse dynamics calculator for each frame. For the calculation of the joint torques we use the Newton Euler recursive inverse dynamics algorithm [27] [28] [29]. This block finds joint torques that are required to produce the desired human like motion. As mentioned earlier, all the joints are actuated in this model. However since the relative motion between the shoulder and the head and neck is not significant, we have taken these joints to be fixed. The output is obtained in the form of a 11-dimensional vector $\tau \triangleq [\tau_1 \quad \tau_2 \quad \tau_3 \quad \tau_4 \quad \tau_5 \quad \tau_6 \quad \tau_7 \quad \tau_8 \quad \tau_9 \quad \tau_{10} \quad \tau_{11}]^T$. As a result of the computations mentioned above, we obtain a sequence of angle and torque vectors for a certain video or marker data sequence.

In the next stage of the system these torque and angle sequence of vectors are used to discriminate the different walking patterns of humans by using ARMA modeling [31] [32] [33] and Dynamic Time Warping (DTW) [31]. Using these techniques we find the distance between the different walking patterns.

3.2 Inverse Dynamics

The inverse dynamics is calculated using the iterative Newton-Euler dynamic formulation [27] [28] [29] which calculates the torque required to generate the given motion of the human model. The inputs to this algorithm are the position, velocity and acceleration $(\Theta, \dot{\Theta}, \ddot{\Theta})$ of the joint angles. The angle vectors are obtained as mentioned in the previous section. The velocity and acceleration vectors are obtained by taking finite differences of the angle vectors once and twice respectively. Along with these, we also need the knowledge of the kinematics and the mass distribution of the model for completing the calculations.

The iterative Newton-Euler dynamic formulation has two parts, an outward loop and an inward loop. At the end of the algorithm we get the torques to be applied at each joint. If the number of links are n, the algorithm can be represented as below.

- **Outward Loop**: Link velocities and accelerations are computed iteratively starting from link 1 to n
- **Inward Loop**: Forces, torques of interaction and the joint actuation torques are computed recursively from link n to link 1

3.2.1 Outward Loop

To calculate the inertial forces acting on each link of the model we have to calculate the rotational velocity and linear and rotational acceleration of the center of masses of each link. This is done by the outward loop starting from link 1 and going upto link n.

The propagation of the rotational velocity is expressed by the following equation,

$$^{i+1}\omega_{i+1} = {}^{i+1}_{i}\mathrm{R}\,{}^{i}\omega_i + \dot{\theta}_{i+1}\,{}^{i+1}\hat{Z}_{i+1} \tag{3.1}$$

The equation for transforming the angular acceleration from one link to the next is given by,

$$^{i+1}\dot{\omega}_{i+1} = {}^{i+1}_{i}\mathrm{R}\,{}^{i}\dot{\omega}_i + {}^{i+1}_{i}\mathrm{R}\,{}^{i}\omega_i \times \dot{\theta}_{i+1}\,{}^{i+1}\hat{Z}_{i+1} + \ddot{\theta}_{i+1}\,{}^{i+1}\hat{Z}_{i+1} \tag{3.2}$$

The linear acceleration for each link is obtained by the following equation,

$$^{i+1}v_{i+1} = {}^{i+1}_{i}\mathrm{R}({}^{i}\dot{\omega}_i \times {}^{i}\mathrm{P}_{i+1} + {}^{i}\omega_i \times ({}^{i}\omega_i \times {}^{i}\mathrm{P}_{i+1}) + {}^{i}\dot{v}_i) \tag{3.3}$$

Linear acceleration for the center of mass of each link is calculated as follows,

$$^{i+1}\dot{v}_{C_{i+1}} = {}^{i+1}\dot{\omega}_{i+1} \times {}^{i+1}\mathrm{P}_{C_{i+1}} + {}^{i+1}\omega_{i+1} \times ({}^{i+1}\omega_{i+1} \times {}^{i+1}\mathrm{P}_{C_{i+1}}) + {}^{i+1}\dot{v}_{i+1} \tag{3.4}$$

Having obtained the linear and angular acceleration of each link we next find the

inertial force and torque acting at the center of mass of each link.

$$^{i+1}F_{i+1} = m_{i+1}{}^{i+1}\dot{v}_{C_{i+1}} \tag{3.5}$$

$$^{i+1}N_{i+1} = {}^{C_{i+1}}I_{i+1}{}^{i+1}\dot{\omega}_{i+1} + {}^{i+1}\omega_{i+1} \times {}^{C_{i+1}}I_{i+1}{}^{i+1}\omega_{i+1} \tag{3.6}$$

This is the end of the outward loop.

3.2.2 Inward Loop

In this section the actual joint torques required for the motion are calculated. The equations in play are based on the force balance and moment balance equations of a link.

From the force balance equation the following iterative relationship can be deduced,

$$^{i}f_i = {}^{i}{}_{i+1}\mathbf{R}^{i+1}f_{i+1} + {}^{i}F_i \tag{3.7}$$

while from the moment balance equation the following iterative relationship can be deduced,

$$^{i}n_i = {}^{i}N_i + {}^{i}{}_{i+1}\mathbf{R}^{i+1}n_{i+1} + {}^{i}\mathbf{P}_{C_i} \times {}^{i}F_i + {}^{i}\mathbf{P}_{i+1} \times {}^{i}{}_{i+1}\mathbf{R}^{i+1}f_{i+1} \tag{3.8}$$

Finally the joint torques for revolute joints are calculated using the following relation-

ship.

$$\tau_i = {}^i n_i{}^{T\,i}\hat{Z}_i \tag{3.9}$$

3.2.3 Simulation of the Inverse Dynamics System

Simulation of the inverse dynamics was carried out in Matlab. For the input to the system we have to manually identify two keyframes, the start frame in which the human is in the double support phase and the end frame in which the human enters the double support phase for the next time. The angle vectors for each frame of this time duration are fed to the inverse dynamics system as input.

3.3 Forward Dynamics

For the forward dynamics [27] [28] [29] it is convenient to express the equation of motion of the model in a state space form that often hides the minute details of the system, but shows the underlying structure of the equation. The dynamic equation can be written in the following form,

$$\tau = M(\Theta)\ddot{\Theta} + V(\Theta, \dot{\Theta}) + G(\Theta) \tag{3.10}$$

where $M(\Theta)$ is the *mass matrix* of the chain, $V(\Theta, \dot{\Theta})$ is a vector of centrifugal and Coriolis terms and $G(\Theta)$ is a vector of gravity terms. Each element of $M(\Theta)$ and $G(\Theta)$ are complex functions of Θ, while each element of $V(\Theta, \dot{\Theta})$ is a complex function of both Θ and $\dot{\Theta}$. To compute the forward dynamics we are using the inverse dynamics algorithm to find the matrix M and vectors V and G. This is a very convenient way of computing the forward dynamics.

Let us denote the inverse dynamics algorithm as *InverseDynamics*$(q, \dot{q}, \ddot{q})$. The algorithm takes the position, velocity and acceleration variables and returns the joint torque values. Therefore we have,

$$\textit{InverseDynamics}(q, \dot{q}, \ddot{q}) = M(\Theta)\ddot{\Theta} + V(\Theta, \dot{\Theta}) + G(\Theta) \tag{3.11}$$

In this equation the variable $\ddot{q}$ is unknown. But if we put $\ddot{q} = 0$ and the gravitational constant $g = 0$ then we can calculate the vector V as follows

$$\textit{InverseDynamics}(q, \dot{q}, 0) = V(\Theta, \dot{\Theta}) \qquad \text{where} g = 0 \tag{3.12}$$

Once we find the vector V, we put the value of $g = 9.81m/s^2$ and $\ddot{q} = 0$ and calculate the G vector as follows

$$G(\Theta) = \textit{InverseDynamics}(q, \dot{q}, 0) - V(\Theta, \dot{\Theta}) \qquad \text{where} g = 9.81m/s^2 \tag{3.13}$$

Finally putting the vectors V and G we compute the matrix $M(\Theta)\ddot{\Theta}$. To compute the matrix we solve the *InverseDynamics* algoritm putting $\ddot{q} = \delta_i$ where δ_i is a vector having the i^{th} element one and all other elements zero to get the i^{th} column of $M(\Theta)\ddot{\Theta}$.

$$M(\Theta)_i = \textit{InverseDynamics}(q, \dot{q}, \ddot{q}) - V(\Theta, \dot{\Theta}) - G(\Theta) \tag{3.14}$$

Once we have calculated the matrices we can iteratively calculate the angle vectors starting from the very first frame. For the first frame we have to assume an initial

condition for the angle vector.

3.3.1 Simulation and Visualization of the Forward Dynamics System

The computation of the forward dynamics is done as mentioned in the previous section. Here the output that we obtain are the angle variations from one keyframe to the next. However for the visualization of the forward dynamics system a different method is used.

For the visualization of the forward dynamics a specific *Simulink* toolbox named *SimMechanics* has been used. In this toolbox we have developed a human body model identical in mass and length distribution as our model described in the previous chapter. Three types of simulations can be done in SimMechanics, *forward dynamics*, *inverse dynamics* and *kinematics*. We have used the forward dynamics part for our visualization purpose. The following figure shows the model that has been developed.

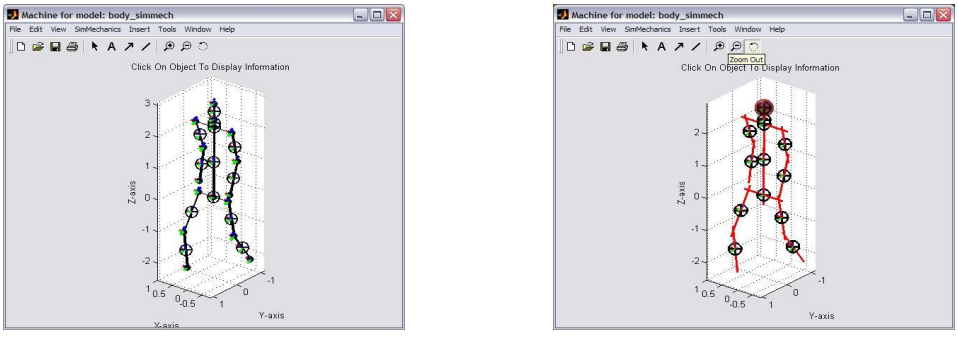

Figure 3.2: Complete human model developed using the SimMechanics toolbox (a) Convex Hull visualization (b) Equivalent ellipsoid visualization

3.3.2 Controller for Forward simulation

The forward dynamics calculation is numerically very unstable and hence the controller [28] is used to stabilize the computations. The controller used in our work is a proportional derivative feedback controller which use the error and error derivative of the angle as the feedback.

3.4 Modeling of Angle and Torque vectors

In this section we provide a brief description of the ARMA modeling and the DTW [31] methods that have been used for finding the similarity been sequences of angle and torque vectors.

3.4.1 ARMA Modeling

We model the torque and the angle sequences as ARMA processes [31] [32] [33]. The dynamical model thus learnt is then used for identification of human gait variations due to loading by calculating the distance between the models. The models thus learnt are continuous state discrete time and since the model parameter lie in a non-Euclidean space the distance calculation is nontrivial.

The ARMA model that has been used is defined as

$$\alpha(t) = Cx(t) + w(t) \qquad \text{where} \quad w(t) \sim N(0, R) \tag{3.15}$$

$$x(t+1) = Ax(t) + v(t) \qquad \text{where} \quad vw(t) \sim N(0, Q) \tag{3.16}$$

The cross correlation between w and v is assumed to be S. It is quite clear that the parameters of the model are A and C. However the matrices A,C,R,Q and S are not unique. Hence we transform the model to the "innovation representation" which is unique.

Given the observation vectors of the torque or angle sequence say $[\alpha(1) \quad \alpha(2) \ldots \alpha(t)]$ we learn the parameters of the innovation representation namely $\hat{A}$, $\hat{C}$ and $\hat{K}$ (Kalman gain matrix) as follows. First we do a singular value decomposition of the data as

$$[\alpha(1) \quad \alpha(2) \ldots \alpha(t)] = U\Sigma V^T \tag{3.17}$$

Then we can say

$$\hat{C}(t) = U \tag{3.18}$$

$$\hat{A} = \Sigma V^T D_1 V (V^T D_2 V)^{-1} \Sigma^{-1} \tag{3.19}$$

where we have $D_1 = [0 \quad 0; I_{t-1} \quad 0]$ and $D_2 = [I_{t-1} \quad 0; 0 \quad 0]$

Distance between two ARMA model is defined in terms of the subspace angles [33] between the two models. The subspace angle between two ARMA models are defined as the principal angles $(\theta_i, i = 1, 2, \ldots, n)$ between the column spaces generated by the observability spaces of the two models augmented with the observability matrices of the inverse models. The Frobenius distance is then defined as

$$d_F = \sqrt{2 \sum_{i=1}^{n} \sin^2 \theta_i} \tag{3.20}$$

and Gap distance is defined as

$$d_g = \sin \theta_{max} \tag{3.21}$$

In our work we have used these two distance measures to quantify the similarity between two ARMA models.

3.4.2 Dynamic time warping

Dynamic time warping is a nonparametric method for comparing two vector sequences. It is basically the best nonlinear time normalization used to match two sequences of vectors by searching the space of all allowed time normalizations. In this implementation we have used some temporal constraints. Further details are provided in [31]. The best warping function and the global warping error are efficiently calculated using dynamic programming.

Chapter 4

Data, Experiments and Results

We have conducted several experiments to judge the validity of our model. This section provides a detailed description of the experiments that we have performed and also the supporting results. Most of the experiments have been done using the marker data collected in the Stanford Biomotion Laboratory. However the same tests can be run on any video data as long as we can extract sufficient information from the video sequence. The information required from the sequence are the joint locations of the human body. A brief description of the Stanford Marker data is also included for ease of reading.

The experiments performed can be broadly divided into three categories. The categories that we have defined for the experiments are as follows.

- Discrimination of Walking Patterns
- Simulation of Walking Patterns
- Validation of the Model using the marker data

4.1 The Stanford Marker Data

This section gives a brief description of the Stanford Marker data used extensively in our experiments. The following figure shows screen shots of a data file that have been visualized.

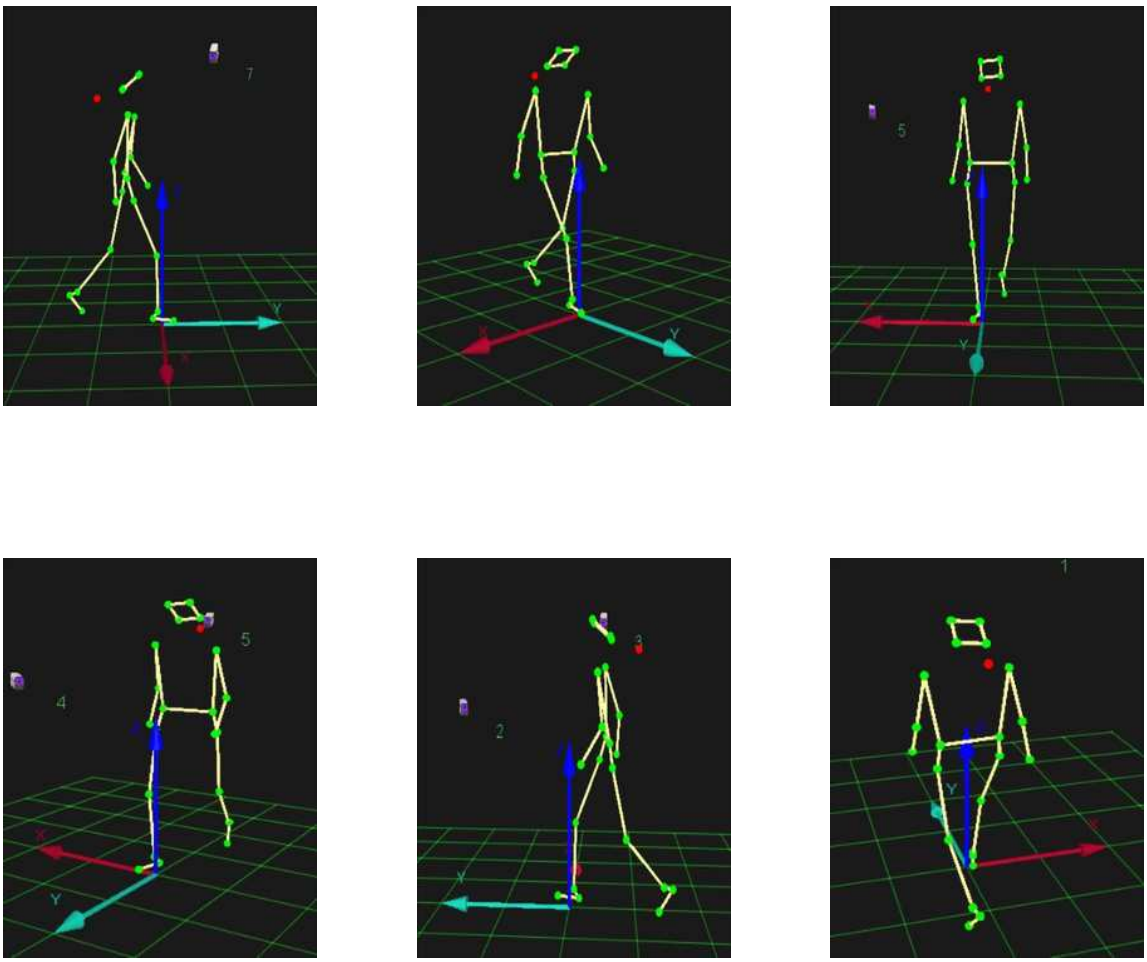

Figure 4.1: Few screenshots of the Stanford Marker Data

The sequences are tracked and the marker positions in 3-D space are obtained. These marker positions are then used to compute the joint angles of the subjects. There are

data corresponding to 6 individuals. Three types walking motion are represented in this dataset.

- Normal Walking
- Walking with a Backpack
- Limping
- Walking with one bare foot

Among these three types of walking, we have used the first three for our experiments for five individuals. For each type of walking and each individual there are 4 sequences. So in our case the dataset contains 60 sequences having 20 sequences of each type of walking. The following table summarizes the dataset.

Number of sequences	Normal Walking	Walking with Backpack	Limping
Individual 1	4	4	4
Individual 2	4	4	4
Individual 3	4	4	4
Individual 4	4	4	4
Individual 5	4	4	4

Table 4.1: Data used in our experiments

4.2 Discrimination of Walking Patterns

In this category of experiments the input to the system is the joint angle data that we receive from the video sequence or the marker data that have been used by us. The first step is extraction of the joint torques from the angle data that is obtained by using the joint locations of the human body. We have used this torque data to discriminate the

different loading conditions of the human body and also to detect any abnormalities in the walking pattern.

The different modeling methods used for the torque data are

1. ARMA modeling

2. Dynamic Time Warping

In both the methods we have tried to find the distance between the torque data that we have received as the output of the system and also the angle data which is the input to the system. As we all know ARMA modeling technique is a well known method for studying time series data and characterizing them. While Dynamic Time Warping involves warping the time axis in order to match two sequences and in the process computes the distance between two time series data.

For ARMA modeling we compute the similarity matrices between different torque and angle sequences using Frobenius and Gap distance. For DTW modeling the global warping error is used as the distance between the models. First few plots show the angle sequences and torque sequences for normal walking, walking with a backpack and limping. The second set of plots illustrate the similarity matrices. All the matrices are 60×60. The first 20 rows/columns correspond to normal walking sequences, next 20 correspond to sequences with backpack and the last 20 correspond to limping sequences. The matrices are shown as images and darker the pixel lesser is the corresponding distance between the models.

The following figures show the results of these experiments.

4.2.1 Results

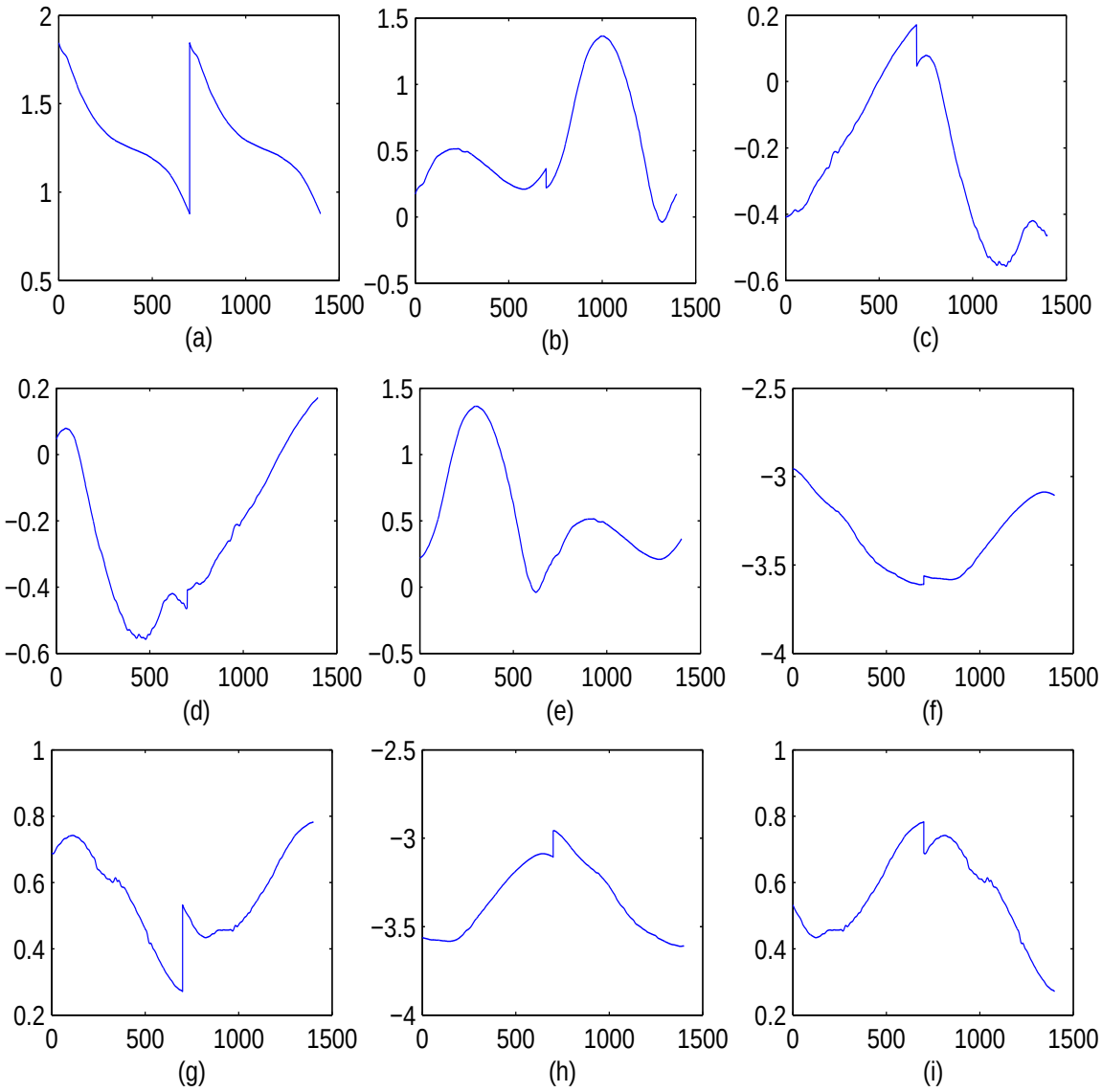

Figure 4.2: The plots of angle data input to the inverse dynamics system block for a single gait cycle. Angle between (a) Ground and the shin of the support leg (b) Right shin and right thigh (c) Right thigh and torso (d) Left thigh and torso (e) Left thigh and shin (f) Torso and left upper arm (g) Left upper arm and lower arm (h) Torso and right upper arm (i) Right upper arm and lower arm

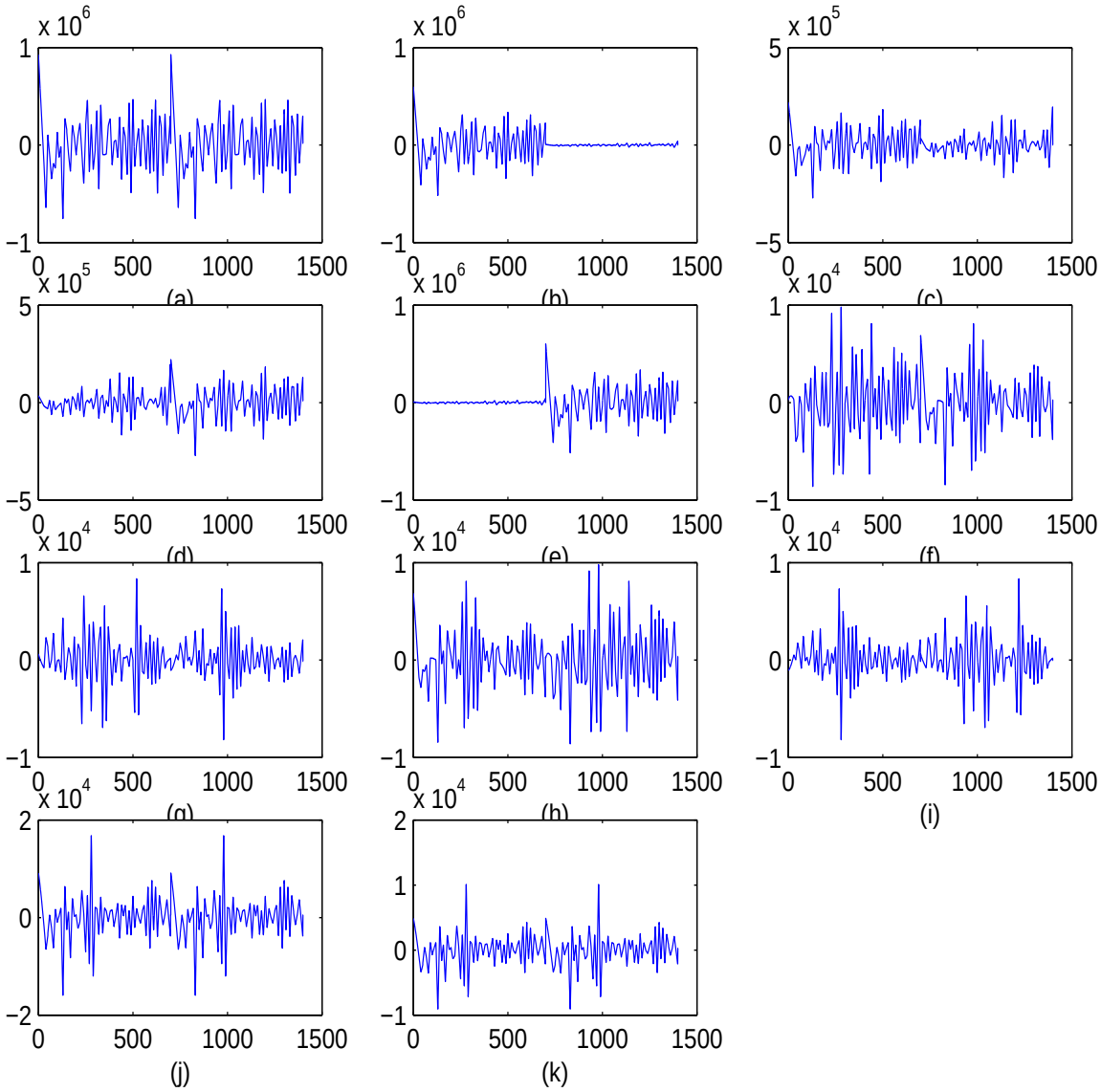

Figure 4.3: The plots of torque data which is the output of the inverse dynamics system block for a single gait cycle. Torque of joint between (a) Ground and the shin of the support leg (b) Right shin and right thigh (c) Right thigh and torso (d) Left thigh and torso (e) Left thigh and shin (f) Torso and left upper arm (g) Left upper arm and lower arm (h) Torso and right upper arm (i) Right upper arm and lower arm (j) Torso and neck (k) Neck and head

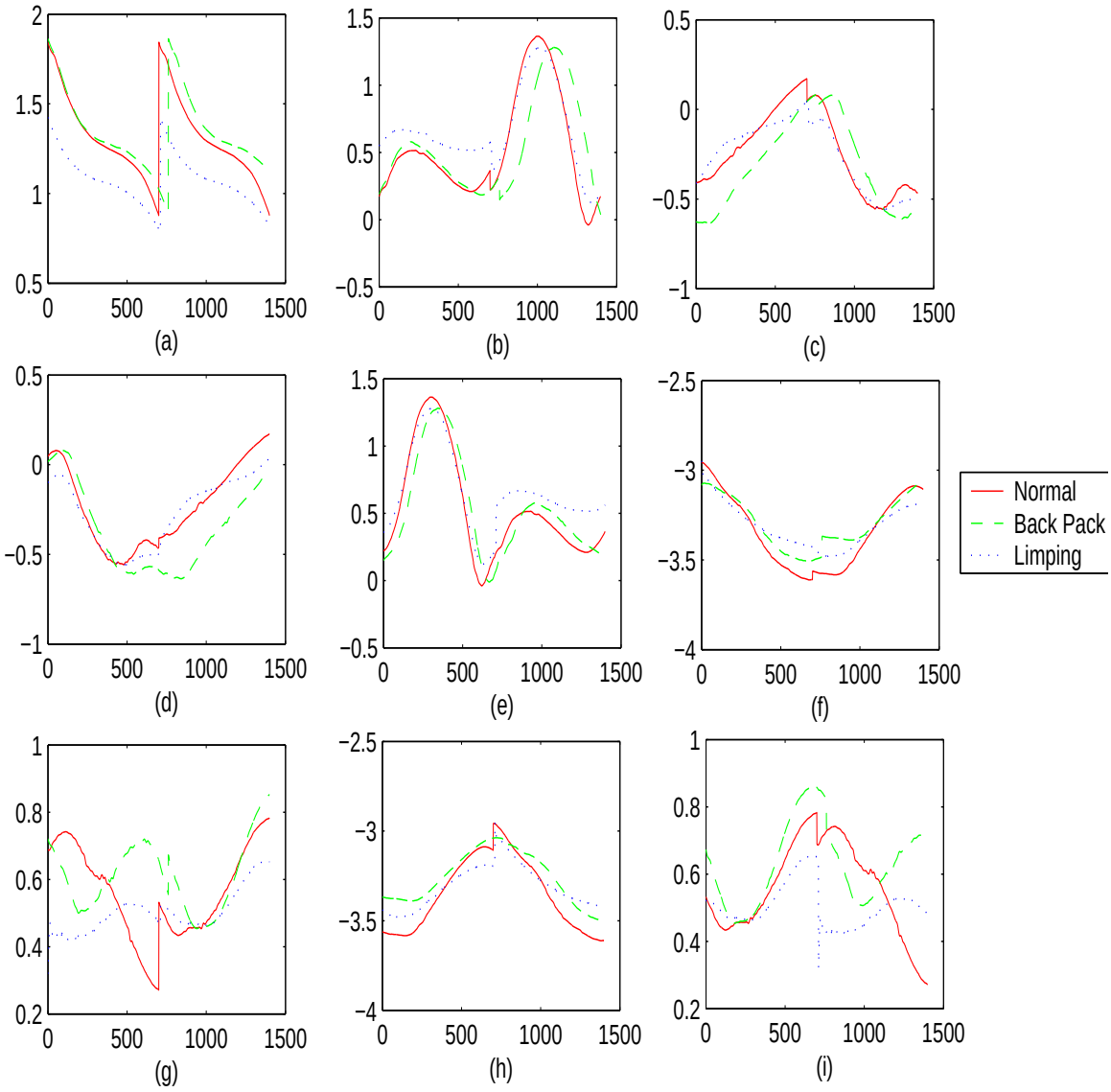

Figure 4.4: The plots of angle data for a normal human, human with a backpack and a limping human, input to the inverse dynamics system block for a single gait cycle. Angle between (a) Ground and the shin of the support leg (b) Right shin and right thigh (c) Right thigh and torso (d) Left thigh and torso (e) Left thigh and shin (f) Torso and left upper arm (g) Left upper arm and lower arm (h) Torso and right upper arm (i) Right upper arm and lower arm

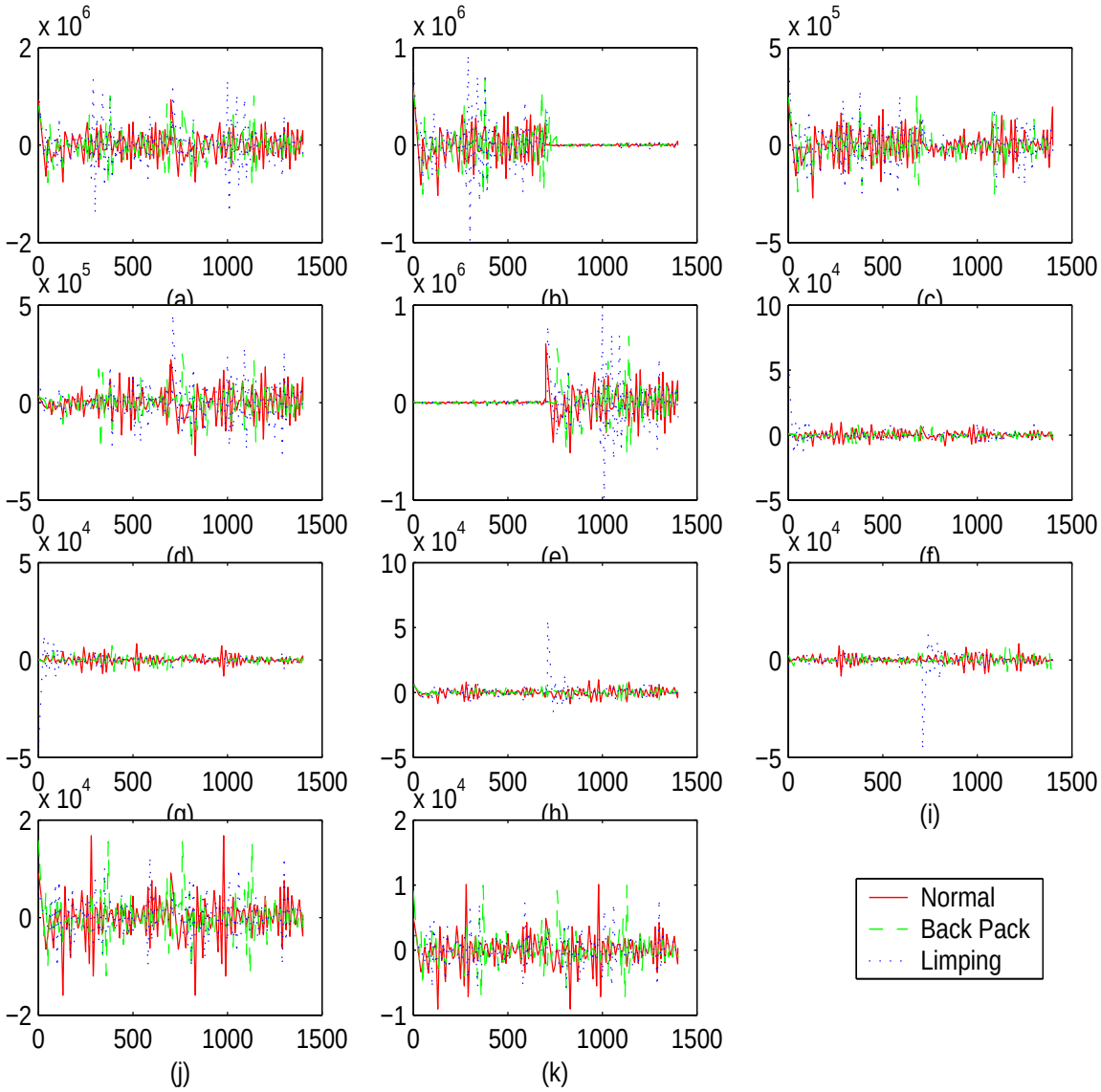

Figure 4.5: The plots of torque data of a normal human, human with backpack and a limping human, which is the output of the inverse dynamics system block for a single gait cycle. Torque of joint between (a) Ground and the shin of the support leg (b) Right shin and right thigh (c) Right thigh and torso (d) Left thigh and torso (e) Left thigh and shin (f) Torso and left upper arm (g) Left upper arm and lower arm (h) Torso and right upper arm (i) Right upper arm and lower arm (j) Torso and neck (k) Neck and head

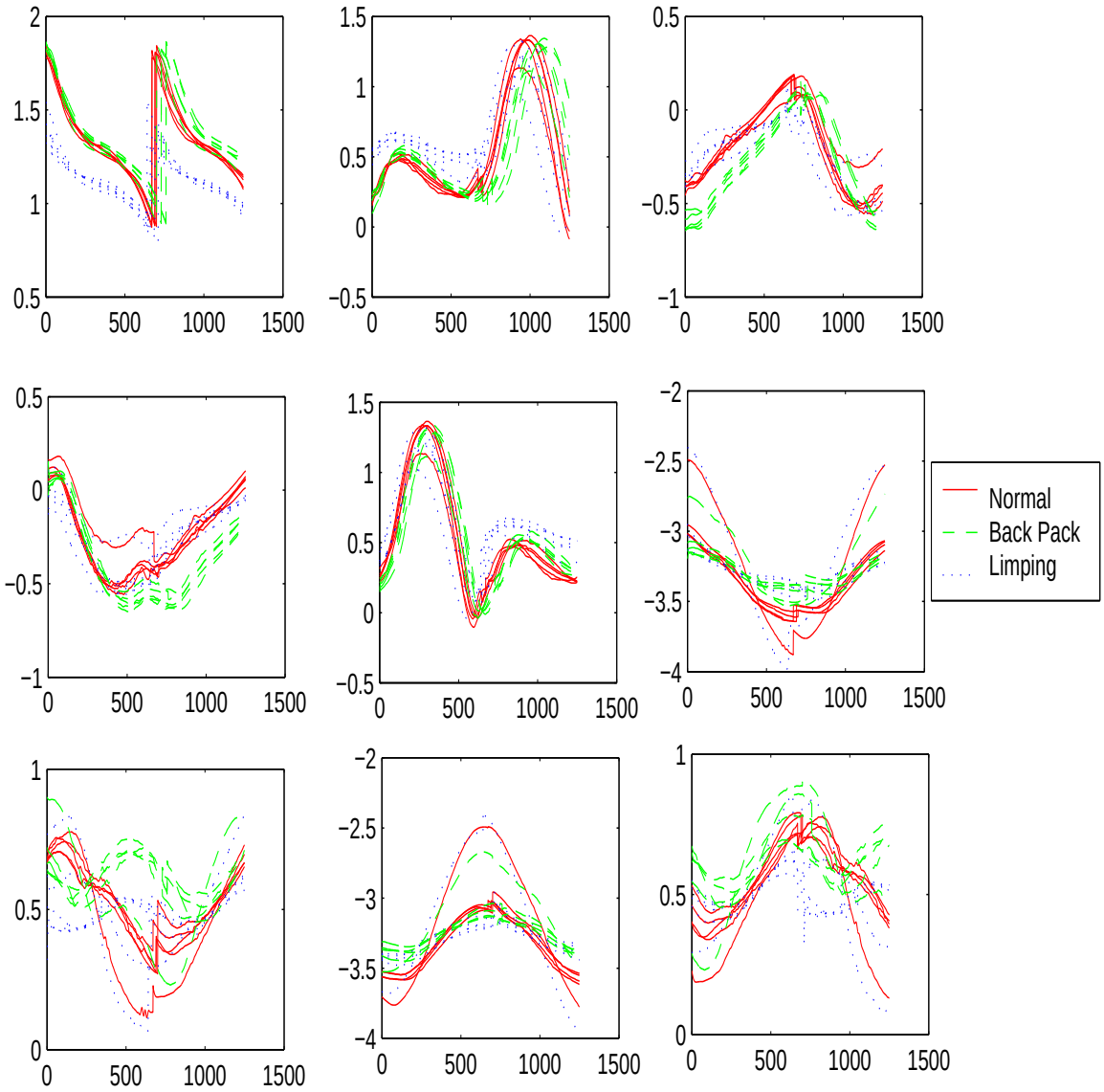

Figure 4.6: The plots of angle data for a normal human, human with a backpack and a limping human, input to the inverse dynamics system block for a single gait cycle and 5 different individuals. Angle between (a) Ground and the shin of the support leg (b) Right shin and right thigh (c) Right thigh and torso (d) Left thigh and torso (e) Left thigh and shin (f) Torso and left upper arm (g) Left upper arm and lower arm (h) Torso and right upper arm (i) Right upper arm and lower arm

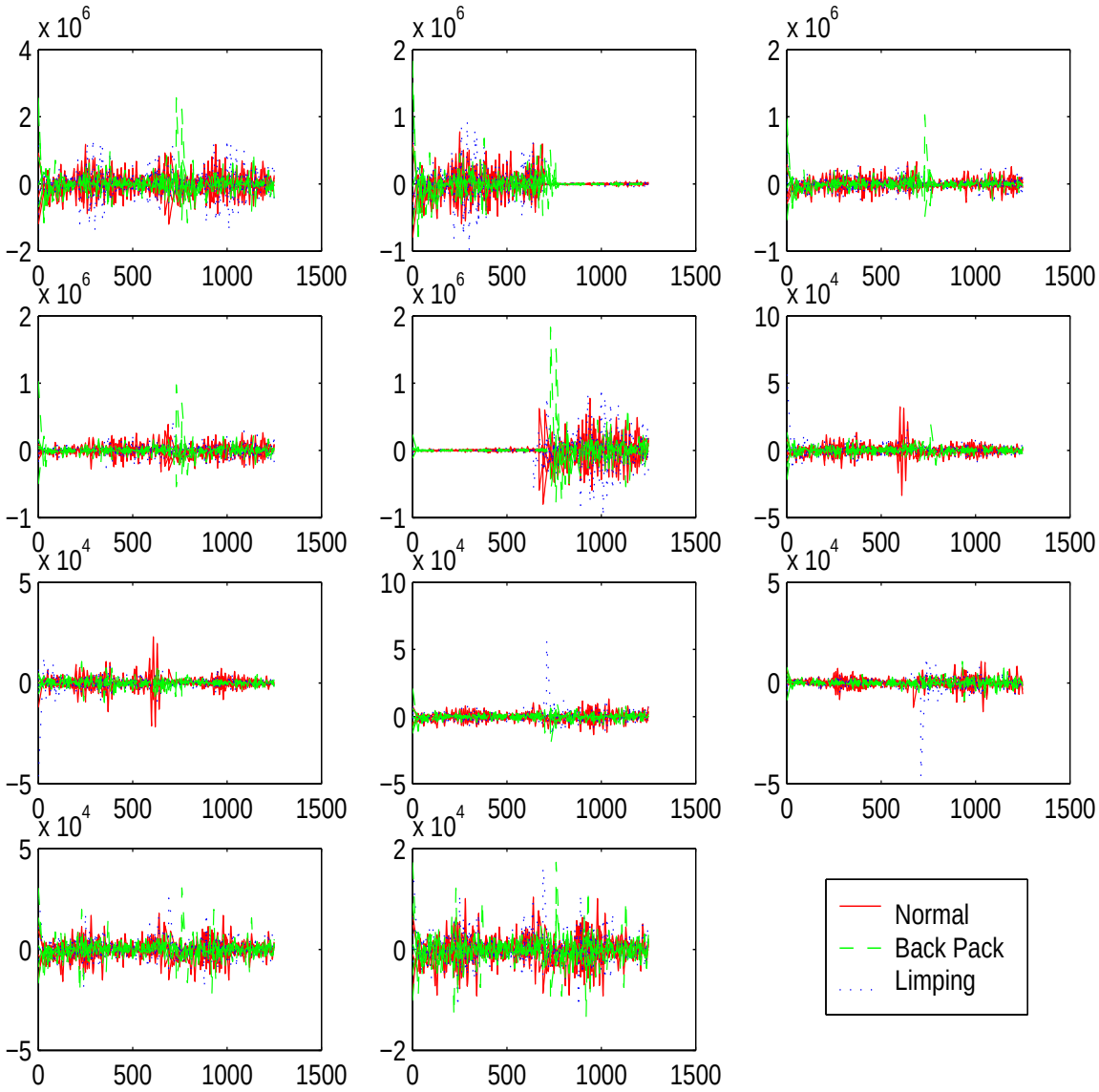

Figure 4.7: The plots of torque data of a normal human, human with a backpack and a limping human, which is the output of the inverse dynamics system block for a single gait cycle and 5 different individuals. Torque of joint between (a) Ground and the shin of the support leg (b) Right shin and right thigh (c) Right thigh and torso (d) Left thigh and torso (e) Left thigh and shin (f) Torso and left upper arm (g) Left upper arm and lower arm (h) Torso and right upper arm (i) Right upper arm and lower arm (j) Torso and neck (k) Neck and head

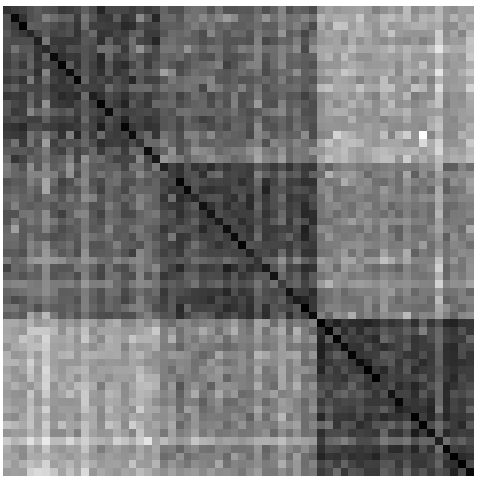

Figure 4.8: The similarity matrix of the angle data using ARMA modeling and gap distance. First 20 are normal, next 20 are with backpack and the last 20 correspond to limping sequences

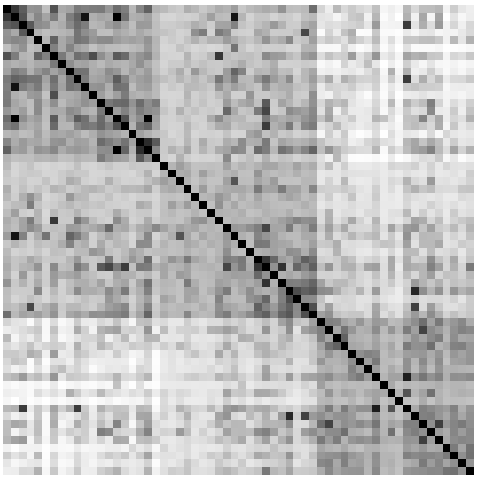

Figure 4.9: The similarity matrix of the torque data using ARMA modeling and gap distance. First 20 are normal, next 20 are with backpack and the last 20 correspond to limping sequences

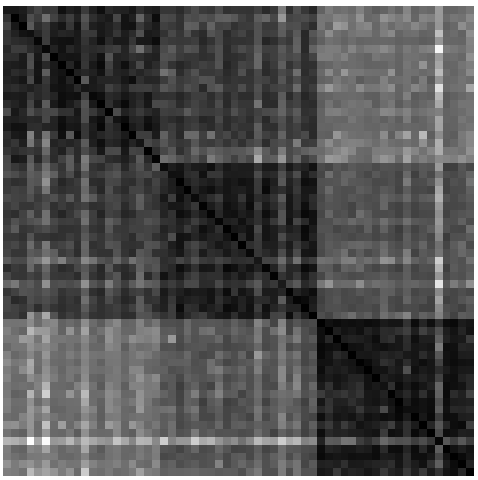

Figure 4.10: The similarity matrix of the angle data using ARMA modeling and Frobenius distance. First 20 are normal, next 20 are with backpack and the last 20 correspond to limping sequences

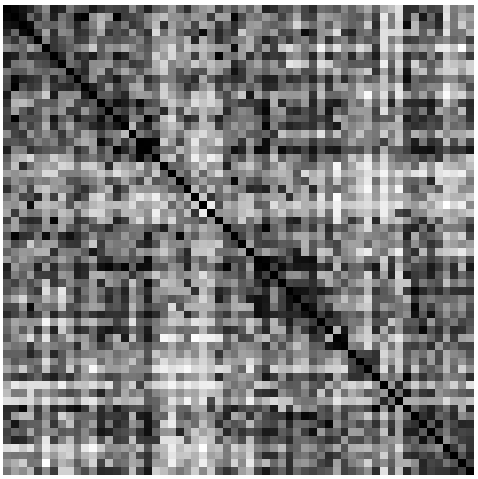

Figure 4.11: The similarity matrix of the torque data using ARMA modeling and Frobenius distance. First 20 are normal, next 20 are with backpack and the last 20 correspond to limping sequences

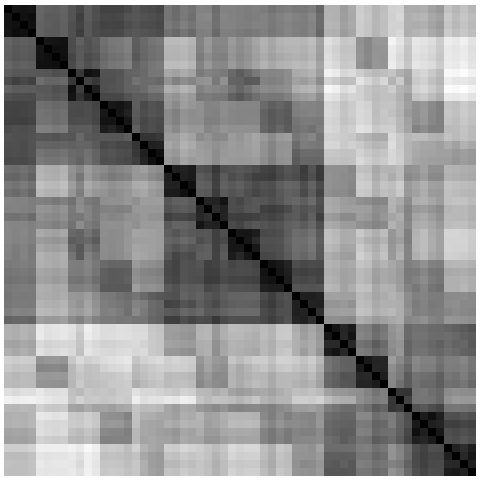

Figure 4.12: The similarity matrix of the angle data using dynamic time warping. First 20 are normal, next 20 are with backpack and the last 20 correspond to limping sequences

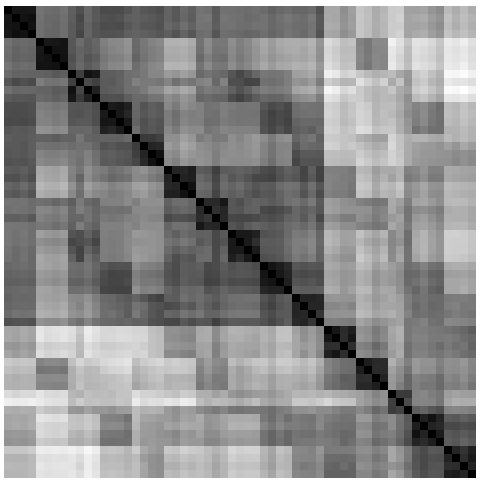

Figure 4.13: The similarity matrix of the torque data using dynamic time warping. First 20 are normal, next 20 are with backpack and the last 20 correspond to limping sequences

4.2.2 Discussion

This section presented the results obtained in the experiments for discriminating different walking patterns. We have tried to distinguish between different types of human walking using the torque and the angle data based on ARMA modeling and Dynamic time warping.

Figures 4.4 and 4.5 show angle and the torque plots respectively for 3 types of walking for the same individual. These plots show good amount of variations between the three walking patterns and these variations are captured by the ARMA modeling and the DTW techniques as shown by similarity matrices in Figures 4.8 to 4.13. Also we observe that when we plot the three different types of torque and angle data for five different individuals the sequences corresponding to similar walking patterns tend to cluster together.

4.3 Simulation of Walking Patterns

In this part of the experiments we have simulated different walking patterns of humans. We simulated the following patterns

- Normal Walking
- Walking with a heavy backpack
- Walking when the Right upper leg is loaded

For the normal walking patterns we have provided the input as the torque sequence obtained in the previous step corresponding to a normal walking sequence. Then we

have visualized and compared the angle sequences obtained as output. While in case of the pattern with a heavy backpack we have increased the weight of the torso of the model considerably so as to simulate the situation of carrying a heavy backpack. The input still remains the same as in the previous step that is the torque sequence corresponding to a normal walking sequence. For the right upper leg loaded condition we have increased the weight of the right upper leg of the model keeping the input same. According to our assumptions and modeling the human model was expected to generate sequences similar to sequences corresponding to normal walking, walking with a heavy backpack and limping. The results of our experiments are quite encouraging and show considerable similarity to the corresponding walking patterns. The following figures show the results of these experiments. For both the backpack and the right leg loading, two loads have been considered to see how the model behaves when the loading is changed. But even if we change the loading, it is observed that the sequences remain similar and cluster together.

The initial plots show the system inputs and the system outputs for different types of walking that is the input torque sequence and the output angle sequences. Some plots also show the torque sequences computed using the angle sequences obtained as output of the forward dynamics simulation. They are considerably similar to the original torque sequences computed from the marker data. The latter part contains the similarity matrices of the torque and the angle data. In this case too we have used both ARMA modeling and DTW.

The following figures show the results of these experiments.

4.3.1 Results

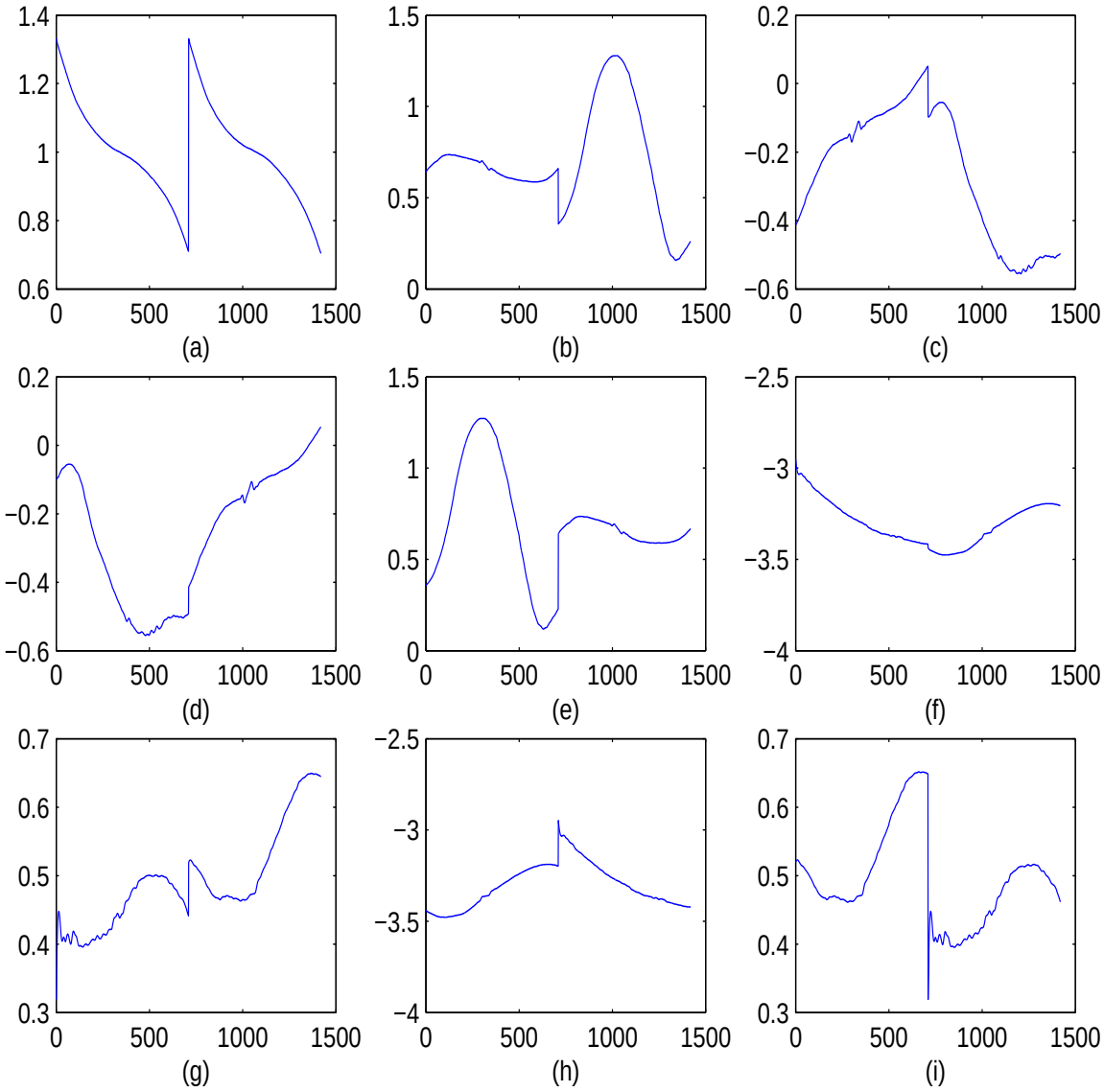

Figure 4.14: Plots of angle data output of the forward dynamics system block for a single gait cycle. Angle between (a) Ground and the shin of the support leg (b) Right shin and right thigh (c) Right thigh and torso (d) Left thigh and torso (e) Left thigh and shin (f) Torso and left upper arm (g) Left upper arm and lower arm (h) Torso and right upper arm (i) Right upper arm and lower arm

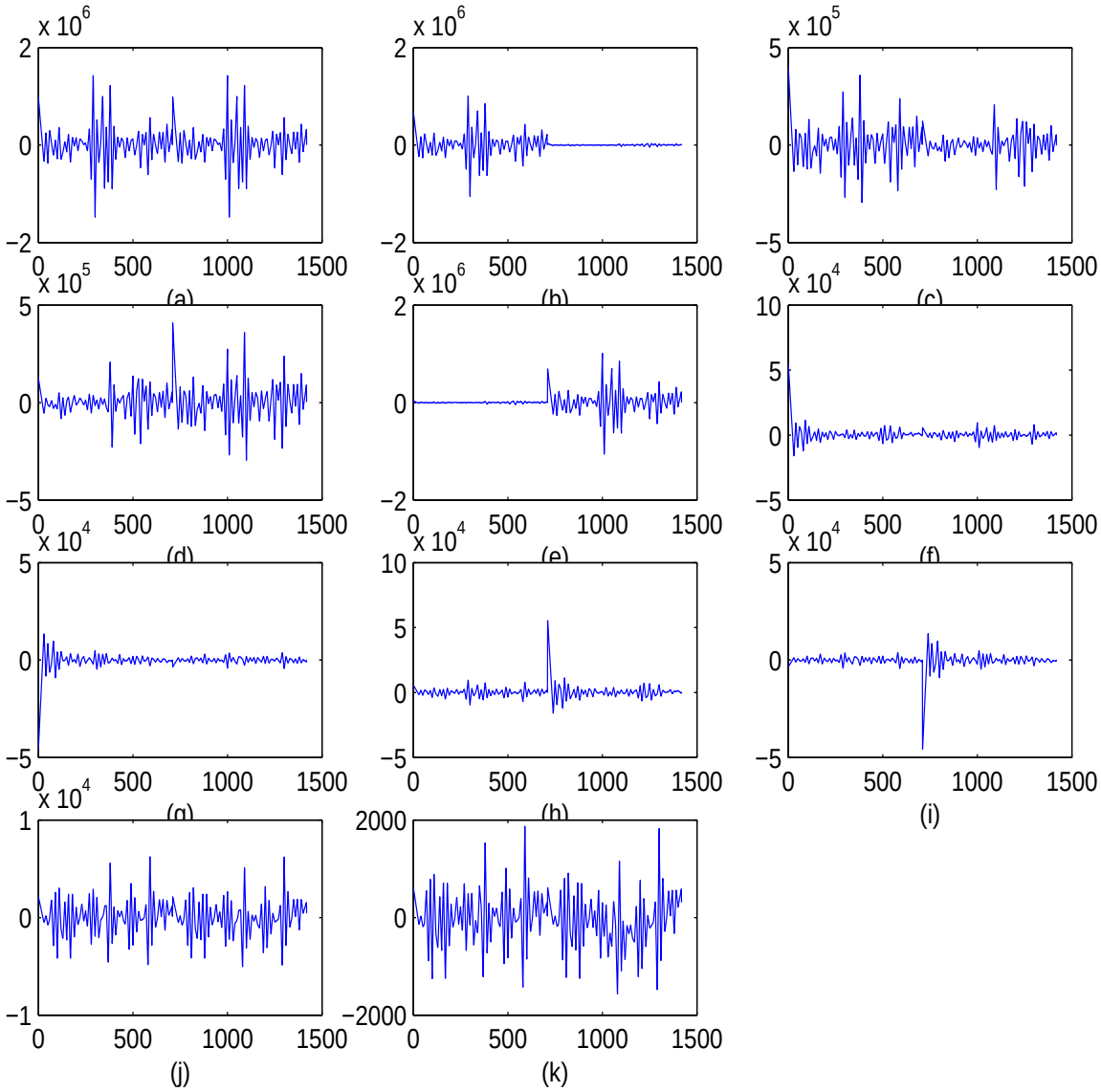

Figure 4.15: Plots of torque data which are input to the forward dynamics system block for a single gait cycle using the controller. Torque of joint between (a) Ground and the shin of the support leg (b) Right shin and right thigh (c) Right thigh and torso (d) Left thigh and torso (e) Left thigh and shin (f) Torso and left upper arm (g) Left upper arm and lower arm (h) Torso and right upper arm (i) Right upper arm and lower arm (j) Torso and neck (k) Neck and head

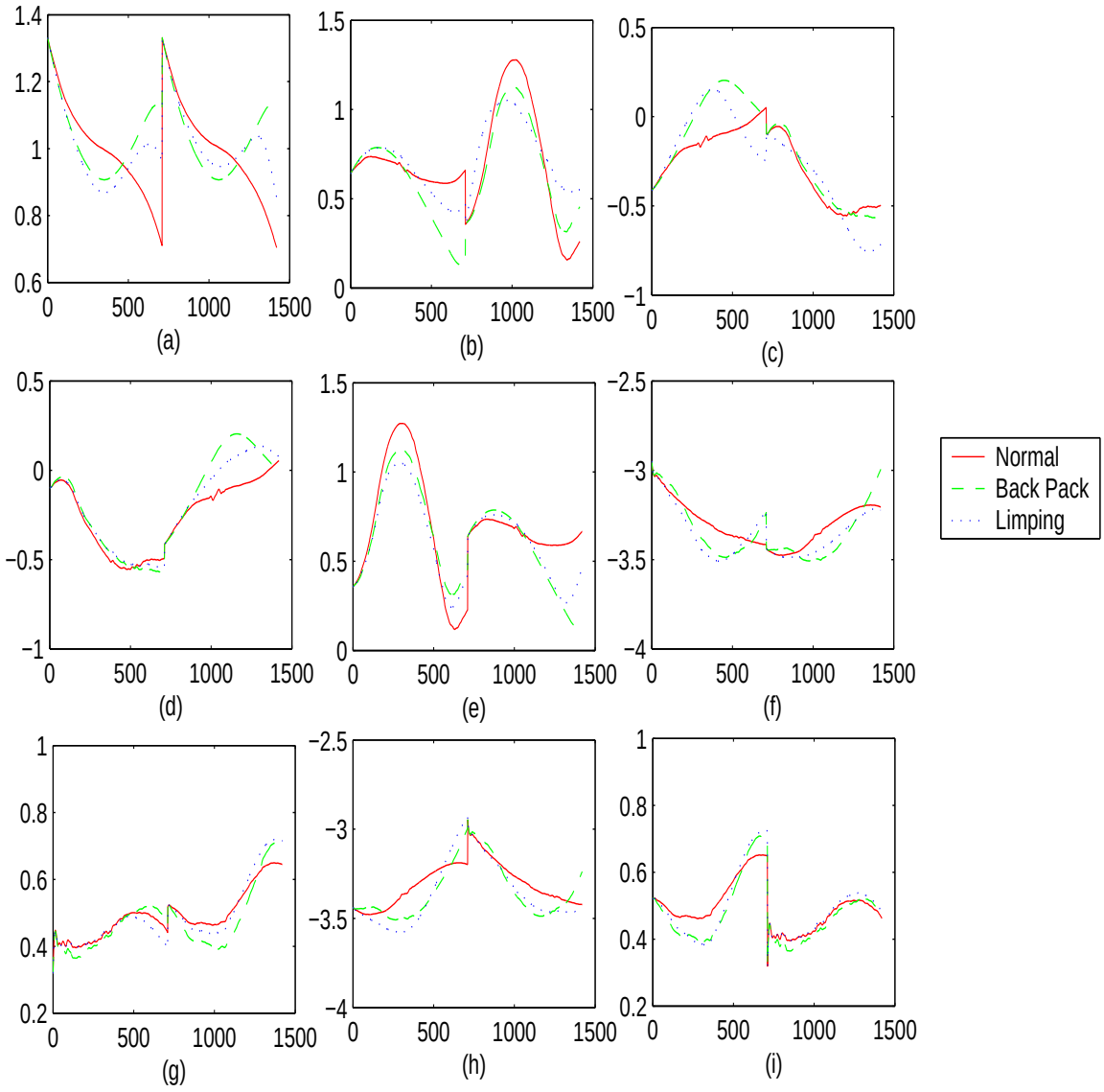

Figure 4.16: Plots of angle data for a normal human, human with a backpack and a limping human, output of the forward dynamics system block for a single gait cycle. Angle between (a) Ground and the shin of the support leg (b) Right shin and right thigh (c) Right thigh and torso (d) Left thigh and torso (e) Left thigh and shin (f) Torso and left upper arm (g) Left upper arm and lower arm (h) Torso and right upper arm (i) Right upper arm and lower arm

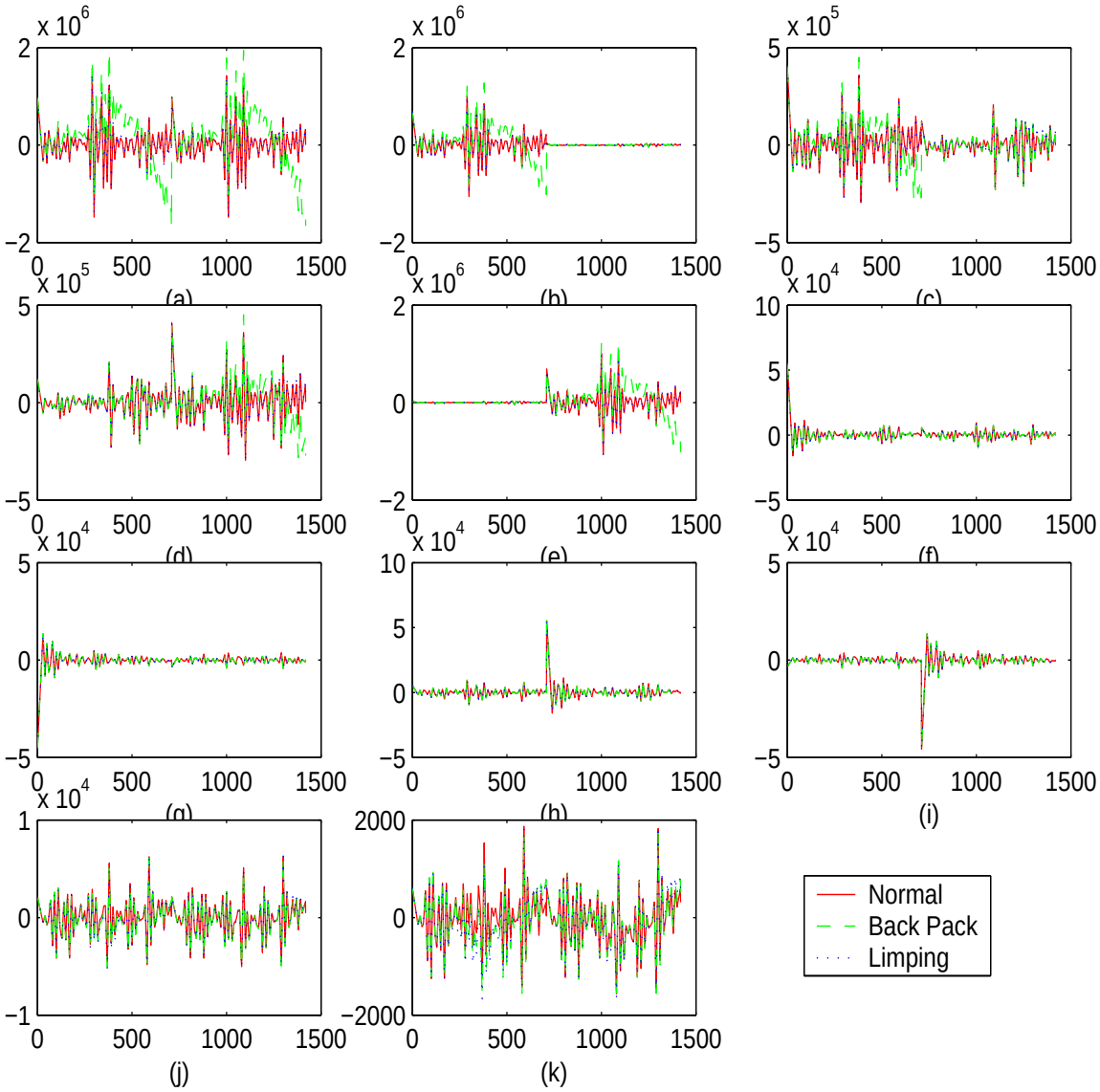

Figure 4.17: Plots of torque data of a normal human, human with backpack and a limping human, which are output to the inverse dynamics system block for a single gait cycle using the controller. Torque of joint between (a) Ground and the shin of the support leg (b) Right shin and right thigh (c) Right thigh and torso (d) Left thigh and torso (e) Left thigh and shin (f) Torso and left upper arm (g) Left upper arm and lower arm (h) Torso and right upper arm (i) Right upper arm and lower arm (j) Torso and neck (k) Neck and head

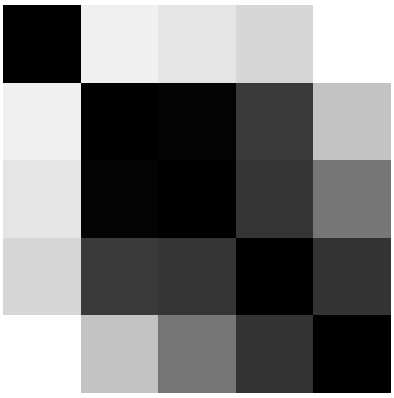

Figure 4.18: The similarity matrix of the angle data using ARMA modeling and Frobenius distance. The first column corresponds to normal walking simulation, the second and the third correspond to walking with a backpack and the last two correspond to limping.

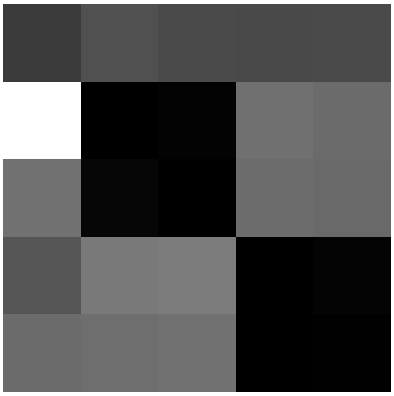

Figure 4.19: The similarity matrix of the torque data using ARMA modeling and Frobenius distance. The first column corresponds to normal walking simulation, the second and the third correspond to walking with a backpack and the last two correspond to limping.

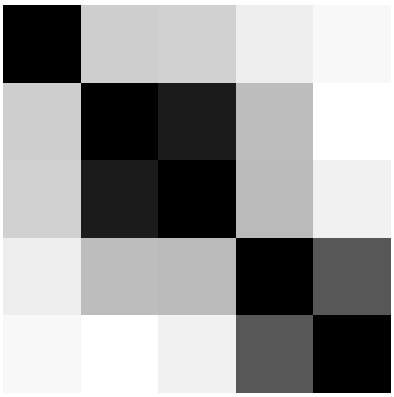

Figure 4.20: The similarity matrix of the angle data using ARMA modeling and Gap distance. The first column corresponds to normal walking simulation, the second and the third correspond to walking with a backpack and the last two correspond to limping.

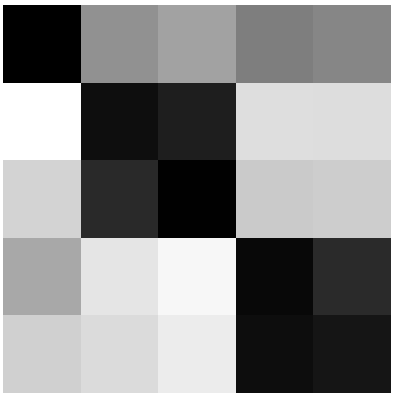

Figure 4.21: The similarity matrix of the torque data using ARMA modeling and Gap distance. The first column corresponds to normal walking simulation, the second and the third correspond to walking with a backpack and the last two correspond to limping.

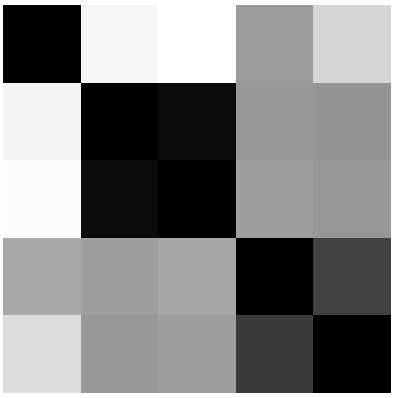

Figure 4.22: The similarity matrix of the angle data using Dynamic time warping. The first column corresponds to normal walking simulation, the second and the third correspond to walking with a backpack and the last two correspond to limping.

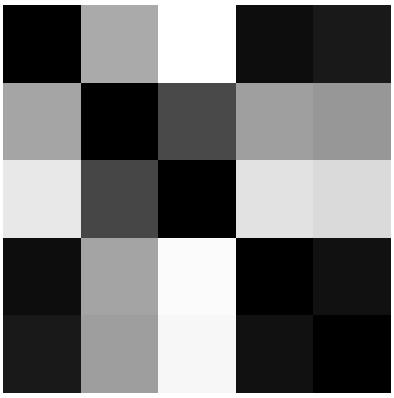

Figure 4.23: The similarity matrix of the torque data using Dynamic time warping. The first column corresponds to normal walking simulation, the second and the third correspond to walking with a backpack and the last two correspond to limping.

4.3.2 Discussion

In this section we have summarized the results of the simulations for generating different walking patterns. Figures 4.14 to 4.17 show the torque and the angle plots. The rest of the figure show the similarity matrices. All the similarity matrices are 5×5. For all the matrices, the first row/column correspond to normal walking. the second and the third correspond to walking with a backpack and the last two correspond to limping.

The important observation of this section is that the outputs are quite well distinguished by the ARMA and DTW modeling. The output video sequences of SimMechanics also show visual confirmation of the variations due to loading. The models react in the expected way with the backpack and also the leg loading conditions.

4.4 Validation of the Model with the marker data

In this section we have compared the output of the model with the marker data to justify the validity of our model. This portion of the results is probably the most important part of the results as this section validates the model.

In this section also we have used ARMA modeling and DTW for comparing the torque and angle sequences obtained from the model and that obtained from the marker data. The figures show the similarity matrices computed using both torque and angle sequences. The columns of the similarity matrices correspond to the data obtained from the model and the rows correspond to that obtained from the marker data. The model data is the one obtained in the previous section and have in all five sequences, the first one correspond to normal walking, the next two correspond to walking with a backpack

and the last two correspond to limping. The 60 rows correspond to the 60 marker sequences. The first 20 correspond to normal walking, the next 20 correspond to walking with a backpack and the last 20 correspond to limping.

The similarity matrices hence have 5 columns and 60 rows. However in the images they are shown as square matrices. The five columns are distinguishable due to the darkening effect of the similarities.

The following figures show the results of these experiments.

4.4.1 Results

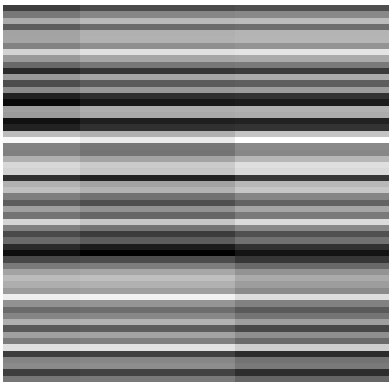

Figure 4.24: The similarity matrix of the angle data of the forward dynamics simulation and the actual marker data using ARMA modeling and Frobenius distance. The first column corresponds to normal walking simulation, the second and the third correspond to walking with a backpack and the last two correspond to limping. The rows correspond to the sixty data sequences. First 20 are normal, next 20 are with backpack and the last 20 are limping sequences.

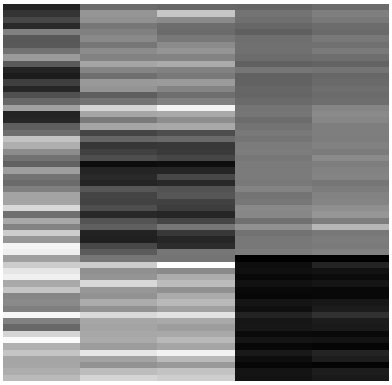

Figure 4.25: The similarity matrix of the torque data of the forward dynamics simulation and output of the Inverse dynamics simulation using ARMA modeling and Frobenius distance. The first column corresponds to normal walking simulation, the second and the third correspond to walking with a backpack and the last two correspond to limping. The rows correspond to the sixty data sequences. First 20 are normal, next 20 are with backpack and the last 20 are limping sequences.

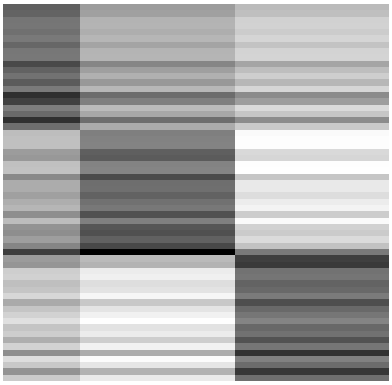

Figure 4.26: The similarity matrix of the angle data of the forward dynamics simulation and the actual marker data using ARMA modeling and Gap distance. The first column corresponds to normal walking simulation, the second and the third correspond to walking with a backpack and the last two correspond to limping. The rows correspond to the sixty data sequences. First 20 are normal, next 20 are with backpack and the last 20 are limping sequences.

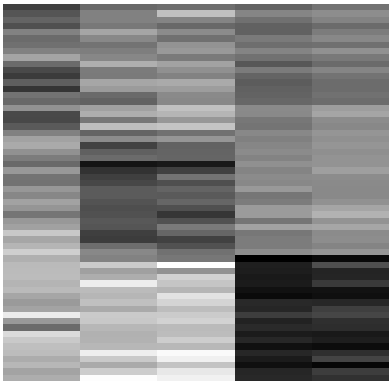

Figure 4.27: The similarity matrix of the torque data of the forward dynamics simulation and output of the inverse dynamics simulation using ARMA modeling and Gap distance. The first column corresponds to normal walking simulation, the second and the third correspond to walking with a backpack and the last two correspond to limping. The rows correspond to the sixty data sequences. First 20 are normal, next 20 are with backpack and the last 20 are limping sequences.

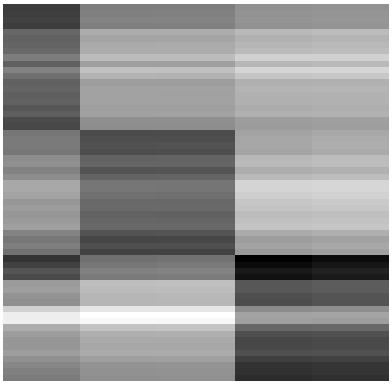

Figure 4.28: The similarity matrix of the angle data of the forward dynamics simulation and the actual marker data using DTW. The first column corresponds to normal walking simulation, the second and the third correspond to walking with a backpack and the last two correspond to limping. The rows correspond to the sixty data sequences. First 20 are normal, next 20 are with backpack and the last 20 are limping sequences.

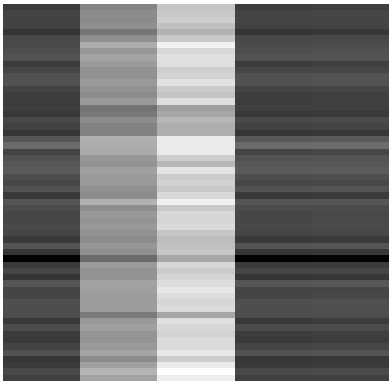

Figure 4.29: The similarity matrix of the torque data of the Forward dynamics simulation and output of the Inverse dynamics simulation using Dynamic time warping. The first column corresponds to Normal walking simulation, the second and the third correspond to walking with a backpack and the last two correspond to limping. The rows correspond to the sixty data sequences. First 20 are normal, next 20 are with backpack and the last 20 are limping sequences.

4.4.2 Discussion

The similarity matrices in this section show that the model closely corresponds to the actual marker data and hence is a valid model to use in discriminating the different walking patterns of humans.

Chapter 5

Conclusion and Future Work

In this thesis we presented a dynamic model for simulating human walking and also identification of some unnatural loading conditions of the walking person. The model consists of an articulated body model made of rigid links connected by joints. The modeling problem has been divided into two different part

- Inverse Dynamic modeling
- Forward Dynamic modeling

The inverse dynamics problem has been solved using the iterative Newton Euler formulation for joint torque computation. We have adopted a model that has in all 11-degrees of freedom. The degrees of freedom are associated with the 11 joints which we consider to be actuated joints. The input to the inverse dynamics system is the joint angle vector obtained from a video sequence or marker data. The output of the system is a 11-dimensional torque vector. This torque vector and also the joint angle vector is then used for identifying any loading like a backpack or something strapped to the leg of the

human body. The work clearly shows that this torque data and also the angle data has discriminative power to identify the loading conditions of the human body as illustrated by the similarity matrices shown in the results section. The similarities were calculated using ARMA modeling and also DTW technique.

In the next part of the work the forward dynamics problem has been solved to generate human gait patterns under different loading conditions. The model has also been validated using the real human marker data by computing the similarity between the artificial gait patterns generated by the forward dynamic model and the Stanford marker data. The artificial patterns show close similarity to the actual human gait data and thus validates the model for use in further research.

There are quite a few modifications and additions that can be done to the model.

- Acquisition of the human joint data from the video sequence needs to be automated so that we can extract the joint data from any unconstrained video data. Presently we have to hand mark the joint positions in the video frames in order to use the model and this is not a practical way of solving the problem.

- The forward dynamics simulation is extremely sensitive to numerical instabilities and more robust algorithms should be used for this portion of the work. This will make the gait pattern generation more accurate and would yield an improved representation for human walking motion.

- Other types of loading conditions should be tried with the model so that we can identify any general condition of the walking human

- Other variations of modeling technique should be tried for the characterization of

torque and angle vectors apart from ARMA modeling and DTW which may lead to better discriminative power and provide us even better results in this area

- The torque and angle vectors can also be tried for human recognition

Bibliography

[1] F. Multon, L. France, M-P. Cani-Gascuel and G. Debunne, Computer Animation of Human Walking: A survey, *SIGGRAPH 90, Conference Proceedings*, pg- 349-358,1990

[2] J.Hodgins, W. Wooten, D. Brogan and J.O'Brien, Animating Human Athletics, *SIGGRAPH 95 Conference proceedings*, pg-71-78, 1995

[3] Y-M. Kang, H-G. Cho and E-T. Lee, An Efficient Control over Human Running Animation with Extension of Planar Hopper Model, *Journal of Visualization and Computer Animation*, 10:215-224, 1999

[4] J. Laszlo, M. van de Panne and E. Fiume, Limit Cycle Control and its Application to the Animation of Balancing and Walking, *SIGGRAPH 96, Conference Proceedings*, pg- 155-162, 1996

[5] J. Laszlo, Controlling Bipedal Locomotion for Computer Animation, *M.S. Thesis*, 1996

[6] M. McKenna and D. Zeltzer, Dynamic Simulation of Autonomous Legged Motion, *SIGGRAPH 90, Conference Proceedings*, pg- 29-38, 1990

[7] A. Bruderlin and T. Calvert, Goal-Directed Dynamic Animation of Human walking,*SIGGRAPH 89, Conference Proceedings*, pg- 233-242, 1989

[8] R. Boulic, N. Thalmann and D. Thalmann, A Global Human Walking Model with Real Time Kinematic Personification, *The Visual Computer*, pg- 344-358, 1990

[9] H. Ko, Kinematic and Dynamic Techniques for Analyzing, Predicting and Animating Human Locomotion, *PhD Thesis*, Department. CIS. University of Pennsylvania, 1984

[10] H. Ko and N. Badler, Animating Human Locomotion in Real-time using Inverse Dynamics, Balance and Comfort control, *IEEE Computer Graphics and Applications*, pg- 50-59, March 1996

[11] N. Badler, C. B. Phillips and B. L. Webber, Simulating Humans: Computer Graphics, Animation and Control, *Oxford University Press*

[12] H. C. Sun and D. N. Metaxas, Automatic Gait Generation,*SIGGRAPH 01, Conference Proceedings*, pg- 261-270, 2001

[13] Y. Hurmuzlu, F. Genot and B. Brogliato, Modeling, stability and Control of Bipedal Robots - A General Framework, *Automatica*, pg- 1647-1664, 2004

[14] Y. Hurmuzlu and G. D. Moskowitz, The Role of Impact in Stability of Bipedal Locomotion, *Dynamics and Stability of Systems*, pg- 217-234, 1986

[15] J. Pratt, C-M Chew, A. Torres, P. Dilworth and G. Pratt, Virtual Model Control: An Intuitive Approach for Bipedal Locomotion, *International Journal of Robotics Research*, Vol. 20, No. 2, pg- 129-143, Feb 2001

[16] C-M Chew and G. Pratt, Adaptation to Load Variations of a Planar Biped: Height Control using robust adaptive control, *Robotics and Autonomous Systems*, pg- 1-22, 2001

[17] A. S. Parseghian, Control of a Simulated, Three-Dimensional Bipedal Robot to Initiate Walking, Continue Walking, Rock Side-to-Side and Balance, *M.S. Thesis*, MIT, 2000

[18] T. Hu, Z. Lin, M. F. Abel and P. E. Allaire, Human Gait Modeling: Dealing with Holonomic Constraints, *The 2004 American Control Conference*, 2004

[19] R. Collins, R. Gross, and J. Shi, Silhouette-based human identification from body shape and gait. *Proc. IEEE Int. Conf. Automatic Face Gesture Recogn.*, May 2002, pg- 351356.

[20] A. Kale, N. Cuntoor, B. Yegnanarayana, A. N. Rajagopalan, and R. Chellappa, Gait analysis for human identification. *Proc. Int. Conf.Audio, Video Biometric Person Authentication*, 2003.

[21] L.Lee and G. Dalley,Learning pedestrian models for silhouette refinement, *Proc. Int. Conf. Comput. Vis.*, 2003, pg- 663670.

[22] A. Sundaresan, A. K. Roy-Chowdhury, and R. Chellappa, A hidden Markov model based framework for recognition of humans from gait sequences, *Proc. Int. Conf. Image Process.*, Sept. 2003.

[23] D. J. Paluska, Design of a Humanoid Biped for Walking Research, *M.S. Thesis*, MIT, 2000

[24] H. Hemami, K. Barin, L. Jalics and D. G. Heiss, Dynamics, Stability and Control of Stepping, *Annals of Biomedical Engineering*, Vol. 32, No. 8, pg- 1153-1160, August 2004

[25] W. T. Dempster and G .Gaughran, Properties of body segments based on size and weight, *American Journal of Anatomy*, 1965.

[26] J-C Cheng and J. M. F. Moura, Capture and Representation of Human Walking in Live Video Sequences, *IEEE Transactions on Multimedia*, Vol. 1, pg- 144-156, June 1999

[27] J. J. Craig, Introduction to Robotics: Mechanics and Control, Second Edition, *Addison-Wesley Publishing Company*

[28] R. M. Murray, Z. Li and S. S. Shastri, A Mathematical Introduction to Robotic Manipulation, *CRC Press*

[29] R. Featherstone, Robot Dynamics Algorithms, *Kluwer Academic Publishers*

[30] K. Yamane, Simulating and Generating Motions of Human Figures, *Springer*

[31] A. Veeraraghavan, A. K. Roy-Chaudhuri and R. Chellappa, Matching Shape Sequences in Video with Applications in Human Movement Analysis, *IEEE Transactions on Pattern Analysis and Machine Intelligence*, Vol. 27, No. 12, pg- 1896-1909, Dec 2005

[32] P. Overschee and B. Moor, Subspace algorithms for the stochastic identification problem, *Automatica*, vol. 29, pg- 649660, 1993.

[33] K. Cock and D. Moor, Subspace angles and distances between ARMA models, *Proc. of the Intl. Symp. of Math. Theory of networks and systems*, 2000.